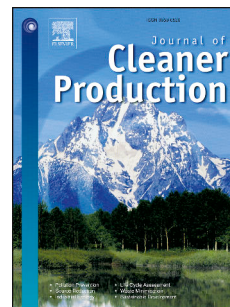


# Journal Pre-proof

Hydrothermal carbonization of microalgae for phosphorus recycling from wastewater to crop-soil systems as slow-release fertilizers

Qingnan Chu, Tao Lyu, Lihong Xue, Linzhang Yang, Yanfang Feng, Zhimin Sha, Bin Yue, Robert J.G. Mortimer, Mick Cooper, Gang Pan



PII: S0959-6526(20)34671-0

DOI: <https://doi.org/10.1016/j.jclepro.2020.124627>

Reference: JCLP 124627

To appear in: *Journal of Cleaner Production*

Received Date: 25 May 2020

Revised Date: 13 September 2020

Accepted Date: 7 October 2020

Please cite this article as: Chu Q, Lyu T, Xue L, Yang L, Feng Y, Sha Z, Yue B, Mortimer RJG, Cooper M, Pan G, Hydrothermal carbonization of microalgae for phosphorus recycling from wastewater to crop-soil systems as slow-release fertilizers, *Journal of Cleaner Production*, <https://doi.org/10.1016/j.jclepro.2020.124627>.

This is a PDF file of an article that has undergone enhancements after acceptance, such as the addition of a cover page and metadata, and formatting for readability, but it is not yet the definitive version of record. This version will undergo additional copyediting, typesetting and review before it is published in its final form, but we are providing this version to give early visibility of the article. Please note that, during the production process, errors may be discovered which could affect the content, and all legal disclaimers that apply to the journal pertain.

© 2020 Elsevier Ltd. All rights reserved.

## Hydrothermal carbonization of microalgae for phosphorus recycling from wastewater to crop-soil systems as slow-release fertilizers

Qingnan Chu<sup>1,2</sup>, Tao Lyu<sup>2,3</sup>, Lihong Xue<sup>1,4,\*</sup>, Linzhang Yang,<sup>1</sup> Yanfang Feng<sup>1,4</sup>,  
Zhimin Sha,<sup>5</sup> Bin Yue,<sup>6</sup> Robert J. G. Mortimer,<sup>2</sup> Mick Cooper,<sup>2</sup> Gang Pan<sup>2\*</sup>

<sup>1</sup>Key Laboratory of Agro-Environment in Downstream of Yangtze Plain, Ministry of Agriculture and Rural Affairs, Institute of Agricultural Resources and Environment, Jiangsu Academy of Agricultural Sciences, Nanjing 210014, China

<sup>2</sup>School of Animal, Rural and Environmental Sciences, Nottingham Trent University, Brackenhurst Campus, Nottinghamshire, NG25 0QF, UK

<sup>3</sup>Cranfield Water Science Institute, Cranfield University, College Road, Cranfield, Bedfordshire, MK43 0AL, UK

<sup>4</sup>School of the Environment and Safety Engineering, Jiangsu University, Zhenjiang, 212001, China

<sup>5</sup>Graduate School of Agriculture and Biology, Shanghai Jiaotong University, Shanghai, 200240, China

<sup>6</sup>College of Geography and Environmental Engineering, Lanzhou City University, Lanzhou, Gansu 730070, China

### Corresponding authors:

\*These authors contribute equally to this work

Prof. Lihong Xue (njxuelihong@gmail.com)

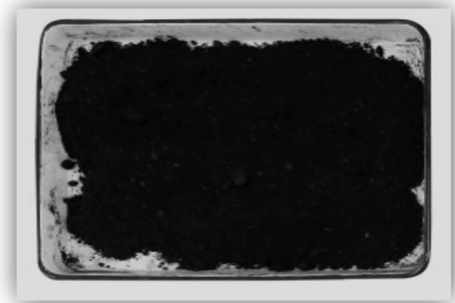
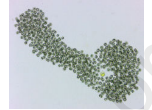
Institute of Agricultural Resources and Environment, Jiangsu Academy of Agricultural Sciences, Nanjing, Jiangsu 210014, China.

Prof. Gang Pan (gang.pan@ntu.ac.uk)

School of Animal, Rural and Environmental Sciences, Nottingham Trent University, Brackenhurst Campus, Nottinghamshire, NG25 0QF, UK



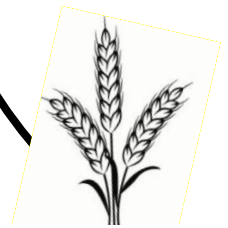
P removal by *Microcystis* sp.  
(88.4% P)



P recycle

Hydrothermal carbonization  
(91.5% P recovery)

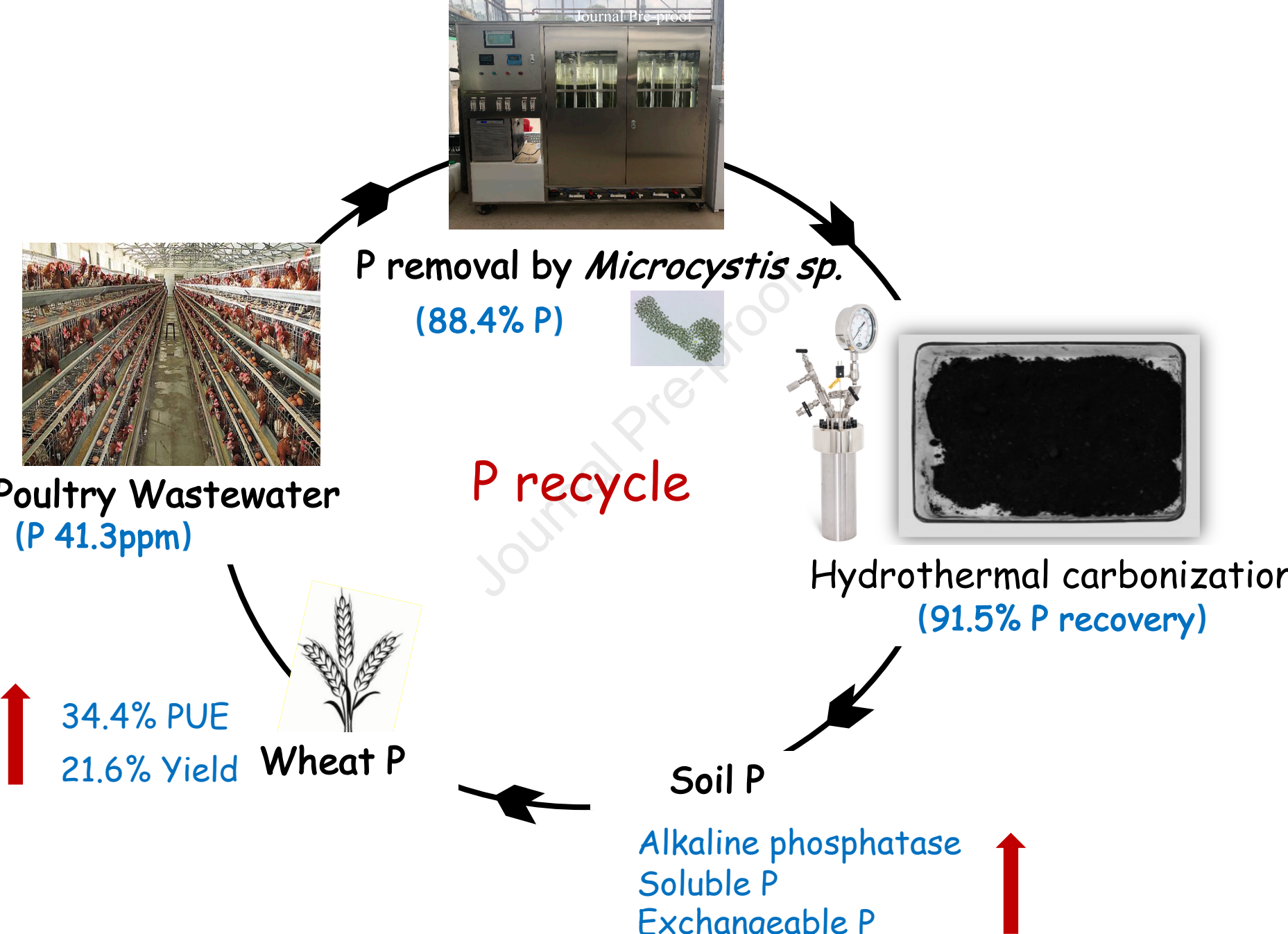
Poultry Wastewater  
(P 41.3ppm)



34.4% PUE  
21.6% Yield ↑  
Wheat P

Soil P

Alkaline phosphatase  
Soluble P  
Exchangeable P ↑



1 **Abstract**

2 Due to the finite stocks of phosphate rock and low phosphorus (P) use efficiency  
3 (PUE) of traditional mineral P fertilizers, more sustainable alternatives are desirable.  
4 One possibility is to culture microalgae in wastewater to recover the P and then  
5 convert the microalgae biomass into slow-release fertilizers through hydrothermal  
6 carbonization (HTC). Therefore, this study aimed to recycle P from wastewater to  
7 agricultural field using microalgae and HTC technology. *Chlorella vulgaris* (CV) and  
8 *Microcystis sp.* (MS) were cultured in poultry farm wastewater with an initial  
9 concentration of 41.3 mg P kg<sup>-1</sup>. MS removed 88.4% P from the wastewater, which  
10 was superior to CV. CV- and MS-derived hydrochars were produced at 200 or 260°C,  
11 in solutions using deionized water or 1wt% citric acid. The MS-derived hydrochar  
12 using 1 wt% citric acid solution at 260 °C (MSHCA260) recovered the highest  
13 amount of P (91.5%) after HTC. The charring promoted the transformation of soluble  
14 and exchangeable P into moderately available P (Fe/Al-bound P), and using citric acid  
15 solution as feedwater increased the P recovery rate and formation of Fe/Al-bound P.  
16 With the abundant moderately available P pool, hydrochar amendment released P  
17 more slowly and enhanced the soil P availability more persistently than chemical  
18 fertilizer did, which helped to improve PUE. In a wheat-cultivation pot experiment,  
19 MSHCA260 treatment improved wheat PUE by 34.4% and yield by 21.6% more than  
20 chemical fertilizer did. These results provide a novel sustainable strategy for recycling  
21 P from wastewater to crop-soil systems, substituting the mineral P fertilizer, and  
22 improving plant PUE.

23 **Keywords:** hydrochar; microalgae technology; phosphorus fractionation; phosphorus  
24 use efficiency; sustainable development; wheat

## 25 **1. Introduction**

26 Phosphorus (P) is an essential plant nutrient and makes up around 0.2% of plant  
27 dry weight (Václavková et al., 2018; Adegbeye et al., 2020). Nevertheless, soil P  
28 exists in pools of low availability and thus becomes one of the major factors limiting  
29 crop growth, affecting approximately 30% agricultural fields worldwide (Xu et al.,  
30 2019; B. Li et al., 2020). Consequently, a vast amount of P fertilizers is required for  
31 agricultural production. However, P-based synthetic fertilizers rely on P extracted  
32 from phosphate rock which is a finite non-renewable resource that might be depleted  
33 in 50-100 years (Withers et al., 2020). In addition, crops take up only 30-45% of the  
34 supplied P from synthetic P fertilizer (Shen et al., 2011; Oita et al., 2020). The P that  
35 is not incorporated into the plants is washed into waterbodies through leaching and  
36 runoff, causing environmental issues (Pan et al., 2018; Lee et al., 2020). Therefore, it  
37 is crucial to seek alternatives to chemical fertilizers and to develop methodologies that  
38 improve P use efficiency (PUE) by crops, while minimizing the negative  
39 environmental impacts.

40 Wastewater contains plentiful P that requires removal prior to discharge into  
41 watercourse. Microalgae have been shown to grow rapidly in such wastewater,  
42 efficiently removing P (Cabanelas et al., 2013; Subramaniyam et al., 2016; Huo et al.,  
43 2020). Microalgae are capable of absorbing inorganic P in excess through storage  
44 within their cells in the form of polyphosphate granules (Delgadillo-Mirquez et al.,  
45 2016)(Solovchenko et al., 2019). Previous studies reported that microalgae can  
46 accumulate large quantities of P (up to 2-4% of their cell dry weight), and thus have  
47 potential to be applied as fertilizer after appropriate processing (Cabanelas et al., 2013;  
48 Santos and Pires, 2018; Luo et al., 2019). Therefore, reclaiming P from wastewater  
49 streams with microalgal cultures is a sustainable and environmental-friendly solution  
50 to the shortage of phosphate rock. In the last decade, direct application of dried  
51 microalgae as an alternative to chemical P fertilizer has been evaluated (Ray et al.,  
52 2013; Mukherjee et al., 2015; Schreiber et al., 2018). A major concern is that the

53 polyphosphate-rich biomass releases the phytoavailable P too slowly into soil to  
54 satisfy the demands of growing plants. Moreover, microalgal toxins, such as  
55 microcystin and cyanotoxin, potentially threatens both soil microbial activity and  
56 plant growth if microalgae are directly applied to soil (Machado et al., 2017). These  
57 factors have driven the researchers to explore additional treatments to enhance the  
58 fertilizer values of microalgal biomass prior to its use in an agricultural context.

59 One such potential tool for increasing PUE is the application of biochar  
60 (Anyaocha et al., 2018; Bornø et al., 2018; Fei et al., 2019; H. Li et al., 2020).  
61 Pyrolysis is the thermal treatment of biomass in absence of air at temperatures of  
62 400-600°C, converting dry biomass into pyrochar (Foong et al., 2020). Hydrothermal  
63 carbonization (HTC) converts wet biomass to hydrochars at lower temperature  
64 (180-260 °C) (Hao et al., 2018; Cui et al., 2020). The higher hydrothermal  
65 temperature than 260°C might lead to the increased generation of noxious compounds  
66 in hydrochars, including phenols and organic acids (Hao et al., 2018). Compared with  
67 pyrolysis, HTC is generally more energy-efficient and, since it is carried out in water,  
68 wet microalgae can be directly processed without prior dehydration (Lachos-Perez et  
69 al., 2017). More importantly, the hydrolysis reaction occurring in HTC process can  
70 promote the degradation of polyphosphate into orthophosphate, with over 90% P  
71 present as orthophosphate in sewage sludge- or manure-derived hydrochars  
72 (Heilmann et al., 2014; Huang and Tang, 2016; Idowu et al., 2017). In addition, the  
73 predominant chemical P fraction in hydrochars is iron (Fe)/ aluminum (Al)-bound P  
74 (Huang and Tang, 2016; Wang et al., 2017), which is considered a moderately labile P  
75 pool for plants and acting as a buffer for available P in soil (Yao et al., 2013;  
76 Heilmann et al., 2014; Fei et al., 2019).

77 Biochar can also improve soil health by increasing soil electrical conductivity  
78 (EC), organic matter content, surface area, and nutrient availability (Bornø et al., 2018;  
79 Yu et al., 2019; Chu et al., 2020c). The microporous structures, surface functional  
80 groups, and intrinsic minerals of hydrochar could improve the capacity of nutrients  
81 adsorption and retention in soil (Yu et al., 2019; Chu et al., 2020a, 2020c), potentially  
82 avoiding P loss and improving plant PUE. Also, remarkable alterations of the

83 microbial community structure in biochar-amended soil have been reported (Ye et al.,  
84 2019; Lu et al., 2020), possibly by affecting phosphatase activity secreted by soil  
85 microorganisms and consequently, by P solubilization. These beneficial properties,  
86 plus the increased moderately labile P pool present within microalgae-derived  
87 hydrochars, are likely to improve the PUE, nutrients retention, and crop growth.

88 This study aims to achieve P recycling from wastewater to food through the  
89 recovery of P from wastewater using microalgae, converting the biomass into  
90 hydrochar by HTC, and applying the microalgae-derived hydrochars to a crop-soil  
91 system. The specific objectives of this work included 1) investigating the fate of P  
92 from wastewater to hydrochar and then to the crop-soil system; 2) screening the most  
93 suitable microalgae-derived hydrochar to improve the PUE compared to traditional  
94 synthetic P fertilizer.

## 95 **2. Methods and materials**

### 96 *2.1. Microalgal cultivation and harvest*

97 *Chlorella vulgaris* strain CCAP 211/12 and *Microcystis sp.* strain CCAP  
98 1450/13 were used in this study and purchased from Culture Collection of Algae and  
99 Protozoa (CCAP), Scottish Marine Institute, Scotland. The wastewater was collected  
100 from the poultry farm at Nottingham Trent University's Brackenhurst Campus and  
101 filtered before culturing microalgae. The trials of P removal from wastewater by  
102 culturing microalgae were carried out in 3 L borosilicate bioreactors in the  
103 glasshouse of Brackenhurst campus, Nottingham Trent University, UK. The culturing  
104 conditions were: constant aeration ( $4 \text{ mL s}^{-1}$ ), photoperiod of 14h:10h light:dark  
105 cycles, at a controlled temperature of  $25 \pm 1^\circ\text{C}$  under cool white fluorescent light of  
106 10000 lux intensity. The chemical characterization of wastewater is shown in **Table**  
107 **S1**. The initial total P (TP) concentration in the wastewater was  $41.3 \text{ mg L}^{-1}$ . Three  
108 replicates were conducted for each microalgal strain. The dry weight (DW) of  
109 microalgae was gravimetrically assessed every two days according to standard  
110 method 2540-D (APHA, AWA, WPCF 1992) and reached the stationary phase in



111 wastewater after 14 days. Also, TP of wastewater was analyzed every two days using  
112 an auto analyzer (AQ400, SEAL Analytical GmbH, Germany) in order to monitor the  
113 P removal rate. At the end of culture total nitrogen (TN) were measured  
114 colorimetrically as nitrate after the water samples had been oxidized and total organic  
115 carbon (TOC) were measured using an organic carbon analyzed by an organic carbon  
116 analyzer (TOC-C<sub>CSN</sub>, Shimadzu). Afterwards, the microalgae were collected by  
117 flocculation. The methods of flocculation were the same as detailed in our previous  
118 study (Li and Pan, 2013), and are included in the Supplementary Information. The  
119 flocculation efficiency of both CV and MS was more than 95% (**Fig. S1**).

## 120 2.2. *Microalgae-derived hydrochars preparation*

121 HTC of microalgae was conducted in a 600 mL Teflon lined stainless steel  
122 hydrothermal reactor (Parr Instruments, Moline, IL, USA), using a solid:liquid ratio  
123 of 1:9 (w/w). The wet microalgal biomass was directly mixed with the feedwater and  
124 the final solid/liquid ratio was calculated based on the moisture content. Eight types  
125 of hydrochars were produced using two different microalgae under two different  
126 feedwaters (deionized water and 1 wt.% citric acid solution) and two different  
127 reaction temperatures (200 and 260 °C). For each run, the reactor was heated to 200  
128 or 260 °C at 3 °C min<sup>-1</sup>, and held at the final temperature for a duration of 2 h. The  
129 pressures originating from feedwater alone at the respective reaction temperatures  
130 were not monitored. The reactor was rapidly cooled down to room temperature using  
131 a recirculating condensing engine. The solid and liquid products were initially  
132 separated by centrifugation and fully gravity-filtered through a 0.45 µm membrane.  
133 The total solid recovery rate was recorded.

## 134 2.3. *Characterization of microalgae-derived hydrochars*

135 The pH of the hydrochars was analyzed using a solid/deionized water ratio of  
136 1:2.5 (w/v). The specific surface area (SSA) and porosity were measured using a  
137 NOVA 1200 analyzer (Anton Paar QuantaTec Inc., Graz, Austria), and were



138 calculated by the Brunauer-Emmett-Teller method (Yu et al., 2019). Total C, H, N,  
139 and S contents were determined using an Elemental Analyzer (EL III; elemental  
140 Analysensysteme GmbH, Germany). Concentrations of metallic elements, including  
141 K, Al, Ca, Fe, and Mg were determined by firstly digesting the hydrochars using  
142 HNO<sub>3</sub> (61%) with hydrogen peroxide and then analyzing the digests using inductively  
143 coupled plasma-optical emission spectrometry (ICP-OES), as described in a previous  
144 study (Chu et al., 2019).

145 The sequential extraction of the microalgae-derived hydrochars were carried out  
146 to evaluate the fractions of P present, following previous studies (Hedley et al., 1982;  
147 Bornø et al., 2018) as shown in **Fig S2**. P fractionation in chars can be separated into  
148 soluble P, exchangeable P, alkaline-dissolved and organic P, acid-dissolved and  
149 organic P, and residual P fractions. The solids were separated from the extract after  
150 each batch of extraction via centrifugation at 8000 g for 5 min, and the supernatant  
151 was filtered using a 0.45 μm membrane filter. The P concentrations in extracts were  
152 analyzed colorimetrically by auto-analyzer. TP concentrations of hydrochars were  
153 calculated by summation of all the P fractions. The P recovery rate was calculated  
154 according to the following formula:

$$155 P_{\text{recover}} = (P_{\text{total}} \times \lambda / P_{\text{feedstock}}) \times 100\%;$$

156 where  $P_{\text{total}}$  is the TP content in the hydrochar,  $P_{\text{feedstock}}$  the TP content in the feedstock,  
157 and  $\lambda$  represents the yield of the hydrochar.

#### 158 2.4. Soil incubation experiment

159 The soil used in the incubation experiment was collected from the top soil of  
160 Embleys farm in the UK (0-15 cm; 29% clay, 42% silt, 29% sand). The soil had the  
161 following basic properties: pH 7.7, organic matter content 2.1%, EC 0.52 mS cm<sup>-1</sup>,  
162 cation exchange capacity (CEC) 2.42 cmol kg<sup>-1</sup>, total N 1.2 g kg<sup>-1</sup>, TP 0.63 g kg<sup>-1</sup>,  
163 total K 3.2 g kg<sup>-1</sup>, Olsen-P 12.1 mg kg<sup>-1</sup>. Soils and hydrochars were air-dried, sieved  
164 through 2 mm mesh, and mixed to ensure a relatively homogeneous distribution. 100  
165 g of the top soil were placed in the 200 mL transparent plastic jars for soil incubation  
166 experiments. The jars were covered with loose lids to allow air circulation but to

167 minimize water evaporation. Treatments were as follows: Untreated soil (no chemical  
168 fertilizers or hydrochars were applied), control (chemical fertilizers were applied), CV  
169 (dried powder of *Chlorella vulgaris*), CVHCA200 (CV-derived hydrochar using 1 wt%  
170 citrate acid solution as feedwater; 200 °C HTC), MS (dried powder of *Microcystis*  
171 *sp.*), MSHCA260 (MS-derived hydrochar using 1 wt% citric acid solution as  
172 feedwater; 260 °C HTC). CVHCA260 and MSHCA260 were selected because they  
173 had the highest P recovery rate of the *Chlorella vulgaris*- or *Microcystis sp.*-derived  
174 hydrochars. The chemical fertilization control contained 500 mg N kg soil<sup>-1</sup> in the  
175 form of NH<sub>4</sub>NO<sub>3</sub>, 100 mg P kg soil<sup>-1</sup> in the form of KH<sub>2</sub>PO<sub>4</sub>, and 300 mg K kg soil<sup>-1</sup>  
176 in the form of K<sub>2</sub>SO<sub>4</sub>. In the hydrochar treatments, the application rate of hydrochars  
177 was 0.5 wt% of the soil and chemical fertilizers were additionally supplemented to  
178 achieve the equivalent rates with the N, P, and K rates used in the chemical  
179 fertilization control. Each treatment comprised four replicates. Incubation lasted for  
180 120 days in an illuminated incubator at 25 °C. The soils were sampled at 0, 10, 30, 50,  
181 80, and 120 days. During the incubation period, deionized water was added every two  
182 days to maintain a field water-holding capacity at 60% (w/w).

### 183 2.5. Wheat pot experiment

184 The experiments used 5L plastic pots, each of four kilograms of air-dried soil  
185 sieved to pass through a 2 mm mesh. A filter paper was placed at the bottom of the  
186 pots to prevent soil loss. Before cultivating wheat, hydrochars were mixed with soil  
187 and the pots were incubated for four weeks in a greenhouse under moderately moist  
188 conditions (60% field water-holding capacity). Wheat seeds were pre-germinated in a  
189 petri dish covered with a filter paper and kept in the dark for three days. After the  
190 preincubation period, five germinated wheat seedlings were carefully transplanted to  
191 each pot and thinned to one after one week. The design of treatments was the same as  
192 described in the soil incubation experiment (2.4). Each treatment comprised four  
193 replicates.

194 The wheat plants were harvested at the tillering (20 days after transplantation)  
195 and maturation stages (120 days after transplantation). In order to satisfy the

196 requirement of sampling at two different growth stages, two batches of experiments  
197 were conducted at the same time. Rhizosphere soil samples were collected by  
198 carefully cleansing the soil from the roots (Chu et al., 2017; Sha et al., 2020). The soil  
199 samples were divided into two parts: one portion was freshly prepared for the  
200 determination of enzyme activity and soil microbial C and P content, and another  
201 portion was air-dried for analysis by sequential P fractionation. In fresh soil samples,  
202 the concentration of microbial biomass C (MBC) and P (MBP) were investigated  
203 using the chloroform fumigation-extraction method (Brookes et al., 1982). Acid and  
204 alkaline phosphatase activities in the soil samples were determined as described in a  
205 previous study (Bornø et al., 2018). In dried soil samples, the soil pH was analyzed in  
206 a slurry of 1:2.5 (w/v, soil to water) using a pH-meter. Soil organic matter (SOM) was  
207 measured using the potassium dichromate oxidation method. Soil total N (TN) was  
208 determined by initially digesting with H<sub>2</sub>SO<sub>4</sub> (98%) and then using the Kjeldahl  
209 method (Chu et al., 2016a). CEC was measured using the compulsive exchange  
210 method with 1.0 M ammonium acetate extraction at pH 7.0 (Brookes et al., 1982).  
211 The analysis of soil P fractionation was same for the hydrochars, as described above  
212 (2.3).

### 213 2.6. Statistical analyses

214 All statistical analyses were performed using SPSS version 23.0 (SPSS Inc.  
215 Chicago, IL, USA). One-way analysis of variance (ANOVA) was used to evaluate the  
216 significant difference at a  $P < 0.05$  probability level with Duncan's multiple range  
217 test.

## 218 3. Results

### 219 3.1. Growth of microalgae and P removal in the wastewater

220 The microbial growth curves were plotted showing the values of biomass (as  
221 dry weight) in wastewater versus time (in days) (**Fig 1**). CV and MS both exhibited  
222 exponential growth and reached a stationary phase after 8 days. After 14 days culture,

223 the biomass (dry matter) of MS reached the maximum value ( $1.14 \text{ g}_{\text{dw}} \text{ L}^{-1}$ ), 8.5%  
224 higher than that of CV (**Table S2**). The average biomass productivities of CV and MS  
225 were  $0.068$  and  $0.071 \text{ g}_{\text{dw}} \text{ L}^{-1} \text{ d}^{-1}$ , respectively. The plot of P removal in the  
226 wastewater versus time (in days) is also shown in **Fig 1**. From 0 to 8 days, the P  
227 concentration in the MS culture declined from  $41.3$  to  $4.8 \text{ mg L}^{-1}$ , with a daily P  
228 removal rate of  $2.95 \text{ mg L}^{-1} \text{ day}^{-1}$ , and in the CV culture from  $41.3$  to  $8.8 \text{ mg L}^{-1}$ ,  
229 with a daily P removal rate of  $2.32 \text{ mg L}^{-1} \text{ day}^{-1}$  (**Table S2**). After 14 days culture, the  
230 maximum P removal rate by MS was  $10.7 \text{ mg L}^{-1} \text{ day}^{-1}$ , which was 23.4% higher  
231 than that of CV (**Table S2**). Overall, after 14 days culture, MS and CV removed 88.4%  
232 and 78.7% P, respectively, from an initial concentration of  $41.3 \text{ mg P L}^{-1}$ ; both  
233 microalgae were demonstrated to be able to remove and enrich P from wastewater  
234 efficiently although MS was superior to CV in this respect. In addition to the P  
235 removal, after 14 days the TN concentration in CV and MS culture declined from  
236  $321.6 \text{ mg L}^{-1}$  to  $182.1$  and  $160.4 \text{ mg L}^{-1}$ , TOC from  $375.2$  to  $53.2$  and  $34.8 \text{ mg L}^{-1}$ ,  
237 respectively, suggesting that with the fast growth the microalgae possibly absorbed  
238 and assimilated the N and C at a high rate from the wastewater as well.

### 239 *3.2. Basic physiochemical characteristics of hydrochars*

240 The physiochemical characteristics of the microalgae and microalgae-derived  
241 hydrochars are displayed in **Table 1**. The microalgae-derived hydrochars using  
242 deionized water as feedwater all exhibited an alkaline pH after processing. Using  
243 citric acid as feedwater markedly neutralized the alkalinity of hydrochars from 7.2-8.5  
244 to 5.7-6.6. With hydrothermal temperature decreasing from  $260 \text{ }^{\circ}\text{C}$  to  $200 \text{ }^{\circ}\text{C}$ , the  
245 lower pH was observed in hydrochars, irrespective of microalgae strain. Transforming  
246 the microalgae into hydrochars decreased the C, H, N, and S concentration,  
247 irrespective of microalgae strain (**Table 1**). As a consequence of the vaporization,  
248 degradation, and dissolution processes of labile fractions occurring during HTC,  
249 elements including C, H, N, and S were partially lost to feedwater, whereas  
250 conservative elements such as P and metals were retained in the hydrochars (**Table 1**  
251 **and 2**). The C concentration in hydrochars using citric acid as feedwater ranged from

252 53.9-66.2%, which is 1.5-6.3% higher than that in hydrochars where deionized water  
253 was used as feedwater, while H and N concentration decreased, resulting in higher  
254 C/N and lower H/C ratio.

255 Moreover, the hydrochars using citric acid as feedwater showed a markedly  
256 higher concentration of metals, including Al, Ca, Fe, and Mg, irrespective of  
257 microalgal strain processed (**Table 1**). The increased abundances of these elements  
258 were possibly beneficial for P bonding in hydrochars. Additionally, as a metal with  
259 high mobility, K in hydrochars showed an opposite trend to other metals. Using citric  
260 acid as feedwater during HTC reduced K accumulation in hydrochars compared to  
261 those when using deionized water. In addition, different reaction conditions during  
262 HTC changed the adsorptive capacity of hydrochars (**Table 1**). When compared to the  
263 raw microalgae, hydrochars markedly increased the SSA and porosity. The SSA for  
264 hydrochars using citric acid as feedwater during HTC ranged from 5.8-6.7 m<sup>2</sup> g<sup>-1</sup>,  
265 which was 16.6-18.2% higher than that in hydrochars using only deionized water as  
266 feedwater.

### 267 3.3. Recovery rate of P in hydrochars

268 As displayed in **Table 2**, the charring process resulted in an increased P content  
269 in the hydrochars. The P content in CV-derived hydrochars ranged from 3.4±0.2–  
270 4.3±0.4 %, which was 23.1-67.9% higher than that of raw CV, and in MS-derived  
271 hydrochars ranged from 4.2±0.3–5.8±0.4%, which was 14.7-72.2% higher than that of  
272 raw MS. Moreover, with increasing hydrothermal temperature from 200 to 260°C the  
273 TP increased from 3.2-4.1% to 3.5-4.1% in CV-derived hydrochars, and from 3.9-5.4%  
274 to 4.5-6.2% in MS-derived hydrochars. In addition, TP in MS-derived hydrochars  
275 varied from 3.9-6.2%, which was 21.9-31.9% higher than that in CV-derived  
276 hydrochars. This result might be attributed to the higher P uptake by MS in  
277 wastewater (**Fig. 1**).

278 With hydrothermal temperature increasing from 200 °C to 260 °C, in contrast  
279 with P recovery, the solid recovery rate of hydrochars declined from 40.7-49.8% to  
280 37.3-45.4% in CV-derived hydrochars, and from 44.6-58.8% to 42.1-55.2% in

281 MS-derived hydrochars. This result might be ascribed to the degradation of polymeric  
282 materials (such as hemicellulose and cellulose) at higher temperatures during HTC.  
283 Moreover, using citric acid solution as feedwater during HTC markedly increased the  
284 hydrochar yield and TP, irrespective of microalgal strain. The solid recovery rate of  
285 microalgae-derived hydrochars using citric acid solution ranged from 41.1-62.0%, but  
286 that of hydrochars using deionized water ranged from 32.3-46.3%. Also, for CV, P  
287 content in CVHCA200 and CVHCA260 was 9.4-27.0% higher than that in  
288 CVHW200 and CVHW260; for MS, P concentration in MSHCA200 and MSHCA260  
289 was 21.6-28.2% higher than that in MSHW200 and MSHW260. The highest P  
290 recovery rate for CV and MS were both attained by using citric acid as feedwater,  
291 72.3% in CVHCA260 and 91.5% in MSHCA260.

#### 292 3.4. Fractionation of P in hydrochars

293 The results of the sequential P fractionation of the microalgae and  
294 microalgae-derived hydrochars are presented in **Fig. 2**. The charring process  
295 significantly reduced soluble, exchangeable, and residual P fractions, but increased  
296 largely the Fe/Al-bound and Ca-bound P fractions. The soluble and exchangeable P  
297 generally correspond to the phytoavailable P. This phytoavailable P constituted 34.0%  
298 of the *Chlorella vulgaris* and 27.9% of the *Microcystis sp.*, whereas less than 20%  
299 was detected in derived hydrochars (e.g., 8.8% in MSHCA260) (**Table S5**).  
300 Additionally, with increasing hydrothermal temperature from 200 to 260 °C, the  
301 soluble P fraction decreased sharply, irrespective of microalgal strains.

302 However, the charring process significantly improved the Fe/Al-bound P  
303 fraction by 2.1-3.4 and 1.7-3.8 fold for CV and MS, and the Ca-bound P fraction by  
304 2.7-4.7 and 1.4-2.5 -fold for CV and MS, respectively (**Fig. 2**). Fe/Al-bound P was the  
305 largest P fraction in microalgae-derived hydrochars, ranging from 32.8-52.7%. In  
306 addition, using citric acid solution as feedwater during HTC significantly increased  
307 the Fe/Al- and Ca-bound P fractions. The Fe/Al- and Ca-bound P in CVHCA200,  
308 CVHCA260, MSHCA200, and MSHCA260 ranged from 15.2-30.5% and 5.8-12.6%,  
309 which was 23.6-64.0% and 7.4-90.9% higher than those in CVHW200, CVHW260,

310 MSHW200, and MSHW260, respectively. Using citric acid solution as feedwater  
311 probably better facilitated the bonding between those metallic elements present and P.

312 Overall, HTC promoted the P transformation from readily available and  
313 recalcitrant fractions to potentially available fractions and using citric acid as  
314 feedwater sharpened such transformation. Fe/Al-bound P occupied 46.2% and 51.5%  
315 in CVHCA260 and MSHCA260, but only 19.5% and 20.1% in the raw CV and MS  
316 (**Table S5**), suggesting that P release in hydrochars will be possibly more sustainable  
317 for satisfying the long-term demand of plant growth.

### 318 *3.5.P release from microalgae-derived hydrochars to soil*

319 The raw microalgae and microalgae-derived hydrochars were incubated in the  
320 soil for 120 days, in order to investigate the release capacity of phytoavailable P, as  
321 shown in **Fig. 3**. The unfertilized soil and soil applied with chemical fertilizers were  
322 regarded as control groups. CVHCA260 and MSHCA260 were selected in this  
323 experiment because of their highest TP (**Table 2**) and highest moderately labile P pool  
324 (**Fig. 2**) among the respective microalgae-derived hydrochars. At 10 days after  
325 incubation, the available P concentration in soils treated with chemical fertilizer was  
326 remarkably and consistently higher than that in other treatments. However, after 50  
327 days, the two hydrochar treatments, CVHCA260 and MSHCA260, significantly and  
328 persistently improved the concentration of soil available P compared to the chemical  
329 fertilizer group. At 120 days after incubation, the soil available P concentration under  
330 CVHCA260 and MSHCA260 treatment was 47.7% and 56.3% higher than that for  
331 the chemical fertilizer group, respectively. In addition, from 10 to 30 days the  
332 available P concentration in soils treated with CV and MS were consistently higher  
333 than those treated with CVHCA260 and MSHCA260, however, an opposite trend was  
334 observed from 30 to 120 days after incubation. At 120 days after incubation, soil  
335 available P concentration under CVHCA260 treatment was 10.9% higher than that  
336 under CV treatment, and under MS260 treatment was 21.0% higher than that under  
337 MS treatment. From 50 to 120 days, the highest soil available P concentration was



338 consistently detected in the MSHCA260 treatment, although a decreasing trend was  
339 detected for all the groups.

### 340 3.6. *Rhizosphere soil properties*

341 The properties of rhizosphere soils amended with microalgae or  
342 microalgae-derived hydrochars at the ripening stage of wheat are shown in **Table S6**.  
343 CVHCA260 and MSHCA260 significantly reduced soil pH by 0.4-1.6 units compared  
344 to the control. CV, MS, CVHCA260, and MSHCA260 significantly improved the  
345 SOM by 19.8%, 12.3%, 25.8%, and 26.6% respectively compared to that in control.  
346 Also, amendment by MSHCA260 significantly improved the CEC compared to the  
347 control and the two microalgae-derived hydrochars significantly improved the CEC  
348 compared to the control, and to the CV- and MS- amended soils. Moreover, with  
349 addition of CV and MS, soil total N was maintained at a similar level to that of the  
350 control, however, amendment by CVHCA260 and MSHCA260 significantly reduced  
351 soil TN by 33.3% and 42.9%, respectively, compared to the control. Because of  
352 effects on SOM and TN, CV and MS addition significantly increased soil C/N ratio  
353 compared to control, by 62.3% and 92.4% for CVHCA260 and MSHCA260  
354 respectively.

355 The incorporation of microalgae and microalgae-derived hydrochars to soil  
356 affected microbial activity, as shown in the results of soil phosphatase activity in **Fig.**  
357 **S3** and MBC and MBP content in **Fig. S4**. The introduction of C from microalgae or  
358 microalgae-derived hydrochars into soil significantly improved the soil MBC,  
359 irrespective of the growth stages, compared to the control. However, soil MBP  
360 displayed different results. At the tillering stage, no significant difference was  
361 detected for MBP, while at the ripening stage, CV and MS addition significantly  
362 reduced MBP by 26.2% and 33.9% compared to the control, and significantly lower  
363 MBP were detected in CVHCA260 and MSHCA260 treatment (reduced 71.9% and  
364 79.5%). Different treatments affected the phosphatase activity in rhizosphere soil. No  
365 significant differences were detected for acidic phosphatase activity among treatments.  
366 However, alkaline phosphatase activity significantly improved either at tillering or

367 ripening stages for CV, MS, CVHCA260, and MSHCA260 treatments when  
368 compared to the control; alkaline phosphate activity in the rhizosphere soil under  
369 CVHCA260 and MSHCA260 treatments was 39.5-42.9% higher than that under CV  
370 and MS treatment at the tillering stage, and 51.7-56.0% higher at the ripening stage.

### 371 3.7. P fractionation in rhizosphere soil of wheat

372 The results of the sequential P fractionation of rhizosphere soil from a wheat pot  
373 experiment are shown in **Fig. 4**. The results of labile and stable P pools in the  
374 rhizosphere soil are shown in **Fig. S5**. Notably, the addition of CV, MS, CVHCA260,  
375 and MSHCA260 significantly reduced soluble P by 4.9-, 3.8-, 3.5-, and 3.6-fold, and  
376 exchangeable P by 47.4%, 82.6%, 80.5%, and 68.3%, respectively, at the tillering  
377 stage. However, an opposite varying trend was observed at the ripening stage; the  
378 addition of CV, MS, CVHCA260, and MSHCA260 increased soil labile P pool (sum  
379 of soluble and exchangeable P fraction) by 1.7-, 1.6-, 1.8-, and 2.1-fold compared to  
380 the control, respectively (**Fig. S5**). Compared to CV and MS, MSHCA260 treatment  
381 resulted in a higher labile P pool at the ripening stage, suggesting that addition of  
382 CVHCA260 could maintain a higher level of soil available P for a longer period.

383 Fe/Al-bound P is defined as the moderate P pool because the P bound to Fe and  
384 Al (hydr)oxides is not directly absorbed by plants but gradually becomes soluble. The  
385 significantly higher Fe/Al-bound P concentrations were detected at the tillering stage  
386 in the soils treated with CV, MS, CVHCA260, and MSHCA260, whereas the opposite  
387 trend was detected at the ripening stage (**Fig. 4C**). In contrast with these treatments,  
388 the Fe/Al-bound P in the control became higher as plants matured, suggesting that, at  
389 an early growth stage of wheat, the readily available P from chemical P fertilizer  
390 became gradually bound to Fe and Al (hydr)oxides. Despite the highest Fe/Al-bound  
391 P concentration (**Fig. 2**) among all hydrochars, the lowest soil Fe/Al-bound P fraction  
392 was detected in the MSHCA260 treatment at the ripening stage (**Fig. 4C**).

393 The sums of Ca-bound P and residual P fractions were defined as the stable P  
394 pool, because Ca-bound P usually corresponds to apatite and residual P corresponds to  
395 recalcitrant P-containing clay mineral (Hedley et al., 1982). Unlike the labile and

396 moderately available P pool, soil Ca-bound and residual P pool kept relatively stable  
397 after the addition of CV, MS, CVHCA260, or MSHCA260 (**Fig. 4D and 4E**). No  
398 significant difference was detected for soil Ca-bound P or residual P fraction among  
399 treatments except at the ripening stage, where addition of MSHCA260 significantly  
400 reduced the soil Ca-bound P fraction compared to the control.

### 401 3.8. PUE and yield of wheat

402 The results of PUE and yields of wheat grain are shown in **Fig. 5**. CV,  
403 CVHCA260, and MSHCA260 treatment significantly improved the plant PUE by  
404 32.4%, 35.3%, and 34.4% compared to the control (**Fig. 5A**). Compared to the raw  
405 CV, amendment by microalgae-derived hydrochars did not significantly improved the  
406 PUE. However, among four treatments only MSHCA260 significantly improved the  
407 wheat grain yield by 21.6% (**Fig. 5B**). In addition, despite statistically insignificant  
408 difference, CVHCA260 treatment improved the grain yield by 14.5% compared to the  
409 control.

## 410 4. Discussions

### 411 4.1. Recovery of P from wastewater and conversion to microalgae-derived hydrochars

412 With the development of “Enhanced biological P removal”, microalgae-based  
413 techniques are attracting increased attention because of the luxury uptake of P by  
414 microalgae, accumulating P up to 2-4% of their cell dry weight (Cabanelas et al.,  
415 2013; Santos and Pires, 2018; Luo et al., 2019). The cost of wastewater treatment  
416 must be counterbalanced with efficacy of P removal and production of microalgal  
417 biomass, which further produces a significant economic benefit to society (Prasad et  
418 al., 2014; Solovchenko et al., 2019). In this study, after 14 days culture in the poultry  
419 wastewater with an initial concentration of 41.3 mg P L<sup>-1</sup>, MS and CV removed 88.4%  
420 and 78.7% P, respectively, showing a strong capacity to remove P from wastewater.

421 **Table S4** compared the P removal efficiencies obtained in this study with the results  
422 in previous studies. This comparison showed that with the increased initial P

423 concentration in influent wastewater the P removal efficiency became higher. In the  
424 present study, MS and CV removed the P from wastewater (with initial P  
425 concentration of 41.3 mg L<sup>-1</sup>) at 2.95 and 2.32 mg L<sup>-1</sup> day<sup>-1</sup>; in previous studies 8.39  
426 mg L<sup>-1</sup> day<sup>-1</sup> P removal rate was observed from the wastewater at initial P  
427 concentration of 128.2 mg L<sup>-1</sup> (Luo et al., 2019) and 0.55 mg L<sup>-1</sup> day<sup>-1</sup> P removal rate  
428 from the wastewater at initial P concentration of 8.0 mg L<sup>-1</sup> (Tao et al., 2017). These  
429 results were likely attributed to the stimulated biosynthesis and storage of  
430 polyphosphate to cope with the external stress of excessive P concentration (Mujtaba  
431 et al., 2017; Shen et al., 2017; Powell et al., 2009; Solovchenko et al., 2016, 2019).

432 Polyphosphate is the dominant P speciation in microalgae (Powell et al., 2009;  
433 Solovchenko et al., 2019) and generally recalcitrant to degradation, making it largely  
434 unavailable for plants. HTC has been demonstrated to be able to promote degradation  
435 by polyphosphate hydrolysis in feedwater. Hence, in the present study the enriched P  
436 in microalgae was transferred to hydrochars by HTC. The P concentrations in  
437 microalgae-derived hydrochars ranged from 3.2-6.2% (**Table 2**), which were notably  
438 higher than hydrochars derived from animal manure and crop residuals (<3%)  
439 (Heilmann et al., 2014; Wang et al., 2017; Fei et al., 2019). This result demonstrated  
440 that luxury P uptake by microalgae from wastewater played an important role in  
441 producing the P-rich hydrochars. In addition, with increasing hydrothermal  
442 temperature from 200 to 260°C, the hydrochar yields were observed to decrease but  
443 the P recovery rate increased, irrespective of feedwater or microalgal strain (**Table 2**).  
444 A similar trend has been reported in the HTC treatment of swine manure (Heilmann et  
445 al., 2014), wetland plants (Cui et al., 2020), and sewage sludge (Huang and Tang,  
446 2016). The cracking of biopolymers and P precipitation during HTC might be  
447 responsible for the higher P accumulation in higher temperature-derived hydrochars  
448 (Dai et al., 2015; Ekpo et al., 2016). The composition of feedwater was demonstrated  
449 to be an important factor for hydrochar yield and P recovery rate. Using 1% citric acid  
450 solution as feedwater significantly improved these parameters, irrespective of reaction  
451 temperature or microalgae strain. Using citric acid solution as feedwater likely  
452 promoted the bonding between metal cations and phosphate. Use of acidic feedwater

453 has previously been demonstrated to promote the release of metal cations in  
454 hydrochars (Idowu et al., 2017; Yuan et al., 2018; Cui et al., 2020) and in the  
455 transformation of organic P to inorganic P (Heilmann et al., 2014; Wang et al., 2017).

456 Differing reaction temperatures and feedwater composition in the HTC process  
457 affected the P fractionation in the resulting hydrochars (**Fig. 2**). The charring of  
458 microalgae significantly reduced the soluble, exchangeable, and residual P fractions,  
459 but increased the Fe/Al-bound and Ca-bound P fractions. Similar results have been  
460 reported where 44.3% readily available P was detected in the raw sewage sludge but  
461 only 7.5% was detected in the derived hydrochars (Fei et al., 2019). During HTC  
462 some orthophosphate dissolved into the feedwater and was lost, whereas most other P  
463 species bonded and adsorbed with various metals to increase retention on the  
464 hydrochars (Zhang et al., 2016). A larger proportion of microalgal P was chemisorbed  
465 by Fe/Al (hydr)oxides compared to that by Ca-containing compounds, which is  
466 comparable with hydrochars derived from sewage sludge (Huang and Tang, 2016; Fei  
467 et al., 2019), but extremely different from animal manure and other plant biomass  
468 where Ca-bound P is dominant (Heilmann et al., 2014; Dai et al., 2015; Bornø et al.,  
469 2018; Cui et al., 2020). Because PAC was used as a reagent to flocculate and collect  
470 the microalgae after culturing in wastewater (**Fig S1**), a larger amount of AlCl<sub>3</sub> was  
471 possibly remained in the microalgae and promoted the formation of the Al-bound P  
472 fractions, as reflected in the Al concentration of hydrochars (0.9-2.8%). Notably,  
473 using 1% citric acid solution as feedwater significantly increased the Fe/Al-bound P  
474 fraction in these hydrochars, irrespective of microalgal strains or reaction temperature,  
475 achieving 46.2% and 51.5% in CVHCA260 and MSHCA260. Importantly, these  
476 Fe/Al-bound P fractions can be desorbed in soil and slowly released as phytoavailable  
477 species (Yao et al., 2013; Heilmann et al., 2014; Fei et al., 2019), avoiding the P  
478 leaching or runoff due to overly fast dissolution, which occurs with chemical P  
479 fertilizer (Koppelaar and Weikard, 2013; Sha et al., 2018; Liu et al., 2020). The  
480 Fe/Al-bound P fractions are considered as moderately available and act as a buffer for  
481 available P in soils (Wang et al., 2014; Zhang et al., 2016; Cui et al., 2020). The loss  
482 of a readily-available P pool during the HTC was more than made up for by a much

483 larger increase in Fe/Al-bound P that eventually can be slowly released into the soil to  
484 support plant growth.

#### 485 *4.2. Application of microalgae-derived hydrochars to a crop-soil system as* 486 *slow-release P fertilizer*

487 Soil incubation and wheat pot experiments both revealed that the  
488 microalgae-derived hydrochars supplied the soil with a pool of slowly-releasable P,  
489 and consequently, the plants with more sustainable P nutrition than did traditional  
490 chemical P fertilizer. In the soil incubation experiment, amendment with CVHCA260  
491 and MSHCA260 persistently improved the soil available P from 50 to 120 days (**Fig**  
492 **3**). In the wheat pot experiment, CVHCA260 and MSHCA260 amendment  
493 significantly improved the soil soluble and exchangeable P fractions (**Fig. 4A and 4B**).  
494 The abundant Fe/Al-bound P pool in hydrochars could be an important reason for the  
495 observed slow-release of P. Sewage sludge-derived hydrochars have been  
496 demonstrated to transform the available P fraction from raw sludge to an Fe/Al-bound  
497 P fraction after HTC, possessing a strong capacity to release P in electrolyte solution  
498 (Huang and Tang, 2016; Fei et al., 2019). Similar results were also reported in the  
499 persistent increase in the soil labile P pool, following amendment with crop  
500 residue-derived biochars (Xu et al., 2016; Bornø et al., 2018). These results suggest  
501 that chemical P fertilizer was beneficial for increasing soil P availability at an early  
502 stage of plant growth whereas microalgae and microalgae-derived hydrochars were  
503 able to supply P to plants over a longer term. However, prior to utilization by plants  
504 the initial pulse of fast-release P from a chemical P fertilizer could possibly be lost by  
505 leaching, runoff, and assimilation by soil organisms, as reflected by the significantly  
506 higher soil MBP in the control (**Fig. S4**).

507 As the wheat grew, it is possible that the pool of moderately available P treated  
508 with microalgae-derived hydrochars gradually transformed to the labile P pool. This  
509 effect is similar with the application of organic and slow-release fertilizer (Chu et al.,  
510 2016b; Václavková et al., 2018). Root activity, leading to the exuding of organic acids  
511 into soil, and phosphatase excreted by soil microorganisms might have driven such

512 transformation (Shen et al., 2018). In the present study, the amendment of  
513 CVHCA260 and MSHCA260 greatly improved the alkaline phosphatase activity in  
514 the rhizosphere both at tillering and ripening stages (**Fig. S3**). HTC promoted the  
515 hydrolysis of macromolecules from microalgae cells, such as polyphosphate and  
516 proteins, to produce a large amount of low weight molecules in the resulting  
517 hydrochars (Bornø et al., 2018; Yu et al., 2019; Chu et al., 2020b). It is speculated that  
518 these low weight molecules were readily assimilated by soil microorganisms and thus  
519 increased microbial activity or, possibly caused a shift in the composition of the  
520 microbial community, resulting in increased levels of alkaline phosphatase,  
521 concomitantly increasing soil available P. Moreover, the charring process significantly  
522 improved the SSA and porosity (**Table 1**). Higher SSA and increased porous volume  
523 levels are extremely important for improving nutrient retention in soil because they  
524 can facilitate higher mass transfer fluxes and adsorption loading of soil nutrients  
525 (Bornø et al., 2018; Chu et al., 2020a; Lu et al., 2020), which might be another reason  
526 for the maintaining higher soil available P over a long term.

527 With the persistently improved soil available P pool in the rhizosphere,  
528 microalgae-derived hydrochar treatments significantly improved plant PUE (**Fig. 5A**).  
529 Notably, however, compared to CV, CVHCA260 and MSHCA260 were observed not  
530 to significantly improve plant PUE. A possible reason might be that improved P  
531 availability due to hydrochar addition exceeded the demand of plant growth. In the  
532 soil incubation experiment, the labile P pool of soils treated with hydrochars were still  
533 far higher than those of most arable soils ( $< 20 \text{ mg kg}^{-1}$ ) and even in excess of the  
534 recommended P application rate (40-50  $\text{mg kg}^{-1}$ ) in agricultural fields (Sha et al.,  
535 2018; Václavková et al., 2018; H. Li et al., 2020). Therefore, in future studies, a  
536 reduced application rate of hydrochars will be attempted. In addition, despite all four  
537 treatments increasing PUE, only MSHCA260 significantly increased the yield of  
538 wheat grain (**Fig. 5B**), perhaps because as well as improved soil P availability,  
539 increases soil C/N, SOM, CEC could also be contributing (**Table S6**). These factors  
540 are beneficial for nutrient mineralization and retention in soil and root morphology  
541 (Shen et al., 2011; Xu et al., 2014; Lu et al., 2020), which might also help promote



542 wheat yield production. In addition, a slightly alkaline soil (pH 7.7) was used in the  
543 present study and the CHVCA260 and MSHCA260 addition lowered the soil pH to  
544 6.4 and 6.6, respectively (**Table S6**). The lowering soil pH was beneficial for  
545 dissolving Ca-bound P and facilitating hydrochars to provide more adsorption sites  
546 between Fe/Al and P compounds. In the present study only deionized water and 1%  
547 citric acid were used as feedwater. In case the feedwater with higher pH is attempted  
548 to produce hydrochars, e.g., 2-5% citric acids, would be acidic and thus possibly  
549 aggravate the soil acidification. Although lowering soil pH might be helpful for the  
550 increase of Fe/Al-bound P pool, the soil acidification is also harmful for root  
551 respiration and growth, as shown in the previous study that poplar sawdust-hydrochar  
552 with pH of 3.7 inhibited rice growth and yield greatly (Yu et al., 2019). Further  
553 studies should carry on to investigate the effects of different feedwater pH on P  
554 recovery in hydrochars.

555 In recent years the synergistic effects of hydrochar application together with  
556 chemical fertilizer on crop yield have been widely reported (Bornø et al., 2018; Yu et  
557 al., 2019; Chu et al., 2020a, 2020c). However, importantly, this study for the first time  
558 demonstrated a substitutive role of hydrochars over chemical P fertilizer to improve  
559 crop production.

## 560 **5. Conclusions**

561 The microalgae, CV and MS, both showed a strong ability for the removal of P  
562 from P-rich wastewater, and MS was superior to CV in this respect. After 14 days  
563 culture in wastewater, MS removed 88.4% P from wastewater at  $2.65 \text{ mg L}^{-1} \text{ day}^{-1}$ .  
564 Then 91.5% P were recovered from the raw MS to the hydrochar MSHCA260. The  
565 P-enriched microalgae-derived hydrochars behaved as a slow-release P fertilizer to  
566 satisfy the long-term demand of growing wheat. MSHCA260 amendment improved  
567 the plant PUE by 34.4% and yield production by 21.6%. The findings from this study  
568 can be used to develop sustainable and eco-friendly strategies to recycle P from  
569 wastewater to agricultural fields for food production, which has the positive dual

570 effects of saving the cost of wastewater treatment and the production of a valuable  
571 slow-release P fertilizer to alleviate the possible future shortage of phosphate rock. A  
572 limitation of the present study is that the microalgal culture was conducted using a  
573 batch experiment under a fixed initial P concentration. The large-scale outdoor  
574 experiments where the influent flow of wastewater keeps feeding are worthy of  
575 carrying out to simulate the industrial wastewater process and quantify the P removal  
576 efficiency by microalgae. Also, the microalgae-derived hydrochars did not improve  
577 significantly the PUE compared to the raw microalgae. Thus, follow-up works are  
578 required to carry out before the large-scale field trials. Further modifications such as  
579 loading metal cations to ameliorate the P chemisorption can be attempted in addition  
580 to using citric acid solution as HTC feedwater.

### 581 **Conflicts of interests**

582 The authors declare no competing financial interest

### 583 **Acknowledgement**

584 We appreciate the funding by National Natural Science Foundation of China  
585 (41807099, 41877090) and Jiangsu Agricultural Science and Technology Innovation  
586 Fund (CX(19)1007). We also acknowledge the financial support of Hunan Zhongke  
587 Water Environmental Management Co., Ltd. And Yantai HABs Control and  
588 Ecological Restoration Technology Co., Ltd through their cooperation projects with  
589 NTU.

### 590 **Author contributions**

591 QC designed the experiments; GP and LX acquired the funding and supervised the  
592 research; QC, TL, BY, and MC performed the experiments; QC analyzed the data; YF  
593 and LY visualized the work; QC wrote the manuscript; TL, RM, LY, and MC  
594 reviewed and edited the manuscript; QC, GP, and LX finalized the manuscript.

595 **Supplementary Information**

596 Detailed information about the materials and methods for microalgae flocculation,  
597 chemical properties of wastewater, the maximum biomass concentration, maximum  
598 biomass productivity, average biomass productivity, maximum P removal rate, and  
599 average P removal rate determined for CV and MS, the concentration of TN, TP, and  
600 TOC in the effluent of wastewater after culturing CV and MS, comparisons between P  
601 removal efficiencies and average P removal rate obtained in this study and previous  
602 studies reporting microalgal in different wastewater effluents, mass content and  
603 relative abundance of different P fractions in raw microalgae and microalgae-derived  
604 hydrochars, the properties of rhizosphere soils amended with microalgae or  
605 microalgae-derived hydrochars at ripening stage of wheat, flocculation efficiency and  
606 zeta potential for flocculating microalgae, overview of the sequential P fractionation  
607 procedure performed on hydrochar and soil samples, acid and alkaline phosphatase  
608 activity in the rhizosphere soil, microbial biomass C and P in the rhizosphere soil,  
609 labile and stable P pool in the rhizosphere soil, are presented in the **Supplementary**  
610 **Information.**

## References

- Adegbeye, M.J., Ravi Kanth Reddy, P., Obaisi, A.I., Elghandour, M.M.M.Y., Oyebamiji, K.J., Salem, A.Z.M., Morakinyo-Fasipe, O.T., Cipriano-Salazar, M., Camacho-Díaz, L.M., 2020. Sustainable agriculture options for production, greenhouse gasses and pollution alleviation, and nutrient recycling in emerging and transitional nations - An overview. *J. Clean. Prod.* <https://doi.org/10.1016/j.jclepro.2019.118319>
- Anyaocha, K.E., Sakrabani, R., Patchigolla, K., Mouazen, A.M., 2018. Critical evaluation of oil palm fresh fruit bunch solid wastes as soil amendments: Prospects and challenges. *Resour. Conserv. Recycl.* <https://doi.org/10.1016/j.resconrec.2018.04.022>
- Bornø, M.L., Eduah, J.O., Müller-Stöver, D.S., Liu, F., 2018. Effect of different biochars on phosphorus (P) dynamics in the rhizosphere of *Zea mays* L. (maize). *Plant Soil* 431, 257–272. <https://doi.org/10.1007/s11104-018-3762-y>
- Brookes, P.C., Powlson, D.S., Jenkinson, D.S., 1982. Measurement of microbial biomass phosphorus in soil. *Soil Biol. Biochem.* [https://doi.org/10.1016/0038-0717\(82\)90001-3](https://doi.org/10.1016/0038-0717(82)90001-3)
- Cabanelas, I.T.D., Ruiz, J., Arbib, Z., Chinalia, F.A., Garrido-Pérez, C., Rogalla, F., Nascimento, I.A., Perales, J.A., 2013. Comparing the use of different domestic wastewaters for coupling microalgal production and nutrient removal. *Bioresour. Technol.* 131, 429–436. <https://doi.org/10.1016/j.biortech.2012.12.152>
- Chu, Q., Sha, Z., Maruyama, H., Yang, L., Pan, G., Xue, L., Watanabe, T., 2019.

Metabolic reprogramming in nodules, roots, and leaves of symbiotic soybean in response to iron deficiency. *Plant. Cell Environ.*

<https://doi.org/10.1111/pce.13608>

Chu, Q., Sha, Z., Nakamura, T., Oka, N., Osaki, M., Watanabe, T., 2016a.

Differential Responses of Soybean and Sorghum Growth, Nitrogen Uptake, and Microbial Metabolism in the Rhizosphere to Cattle Manure Application: A Rhizobox Study. *J. Agric. Food Chem.* 64, 8084–8094.

<https://doi.org/10.1021/acs.jafc.6b03046>

Chu, Q., Sha, Z., Osaki, M., Watanabe, T., 2017. Contrasting Effects of Cattle

Manure Applications and Root-Induced Changes on Heavy Metal Dynamics in the Rhizosphere of Soybean in an Acidic Haplic Fluvisol: A Chronological Pot Experiment. *J. Agric. Food Chem.* 65, 3085–3095.

<https://doi.org/10.1021/acs.jafc.6b05813>

Chu, Q., Watanabe, T., Shinano, T., Nakamura, T., Oka, N., Osaki, M., Sha, Z.,

2016b. The dynamic state of the ionome in roots, nodules, and shoots of soybean under different nitrogen status and at different growth stages. *J. Plant Nutr. Soil Sci.* 179, 488–498. <https://doi.org/10.1002/jpln.201600059>

Chu, Q., Xu, S., Xue, L., Liu, Y., Feng, Y., Yu, S., Yang, L., Xing, B., 2020a.

Bentonite hydrochar composites mitigate ammonia volatilization from paddy soil and improve nitrogen use efficiency. *Sci. Total Environ.*

<https://doi.org/10.1016/j.scitotenv.2020.137301>

Chu, Q., Xue, L., Cheng, Y., Liu, Y., Feng, Y., Yu, S., Meng, L., Pan, G., Hou, P.,

- Duan, J., Yang, L., 2020b. Microalgae-derived hydrochar application on rice paddy soil: Higher rice yield but increased gaseous nitrogen loss. *Sci. Total Environ.* <https://doi.org/10.1016/j.scitotenv.2020.137127>
- Chu, Q., Xue, L., Singh, B.P., Yu, S., Müller, K., Wang, H., Feng, Y., Pan, G., Zheng, X., Yang, L., 2020c. Sewage sludge-derived hydrochar that inhibits ammonia volatilization, improves soil nitrogen retention and rice nitrogen utilization. *Chemosphere* 245, 125558. <https://doi.org/10.1016/j.chemosphere.2019.125558>
- Cui, X., Lu, M., Khan, M.B., Lai, C., Yang, X., He, Z., Chen, G., Yan, B., 2020. Hydrothermal carbonization of different wetland biomass wastes: Phosphorus reclamation and hydrochar production. *Waste Manag.* <https://doi.org/10.1016/j.wasman.2019.10.034>
- Dai, L., Tan, F., Wu, B., He, M., Wang, W., Tang, X., Hu, Q., Zhang, M., 2015. Immobilization of phosphorus in cow manure during hydrothermal carbonization. *J. Environ. Manage.* <https://doi.org/10.1016/j.jenvman.2015.04.009>
- Delgadillo-Mirquez, L., Lopes, F., Taidi, B., Pareau, D., 2016. Nitrogen and phosphate removal from wastewater with a mixed microalgae and bacteria culture. *Biotechnol. Reports.* <https://doi.org/10.1016/j.btre.2016.04.003>
- Ekpo, U., Ross, A.B., Camargo-Valero, M.A., Fletcher, L.A., 2016. Influence of pH on hydrothermal treatment of swine manure: Impact on extraction of nitrogen and phosphorus in process water. *Bioresour. Technol.* <https://doi.org/10.1016/j.biortech.2016.05.012>
- Fei, Y. heng, Zhao, D., Cao, Y., Huot, H., Tang, Y. tao, Zhang, H., Xiao, T., 2019.

Phosphorous retention and release by sludge-derived hydrochar for potential use as a soil amendment. *J. Environ. Qual.* 48, 502–509.

<https://doi.org/10.2134/jeq2018.09.0328>

Foong, S.Y., Liew, R.K., Yang, Y., Cheng, Y.W., Yek, P.N.Y., Wan Mahari, W.A., Lee, X.Y., Han, C.S., Vo, D.V.N., Van Le, Q., Aghbashlo, M., Tabatabaei, M., Sonne, C., Peng, W., Lam, S.S., 2020. Valorization of biomass waste to engineered activated biochar by microwave pyrolysis: Progress, challenges, and future directions. *Chem. Eng. J.* <https://doi.org/10.1016/j.cej.2020.124401>

Hao, S., Zhu, X., Liu, Y., Qian, F., Fang, Z., Shi, Q., Zhang, S., Chen, J., Ren, Z.J., 2018. Production Temperature Effects on the Structure of Hydrochar-Derived Dissolved Organic Matter and Associated Toxicity. *Environ. Sci. Technol.* <https://doi.org/10.1021/acs.est.7b04983>

Hedley, M.J., Stewart, J.W.B., Chauhan, B.S., 1982. Changes in Inorganic and Organic Soil Phosphorus Fractions Induced by Cultivation Practices and by Laboratory Incubations. *Soil Sci. Soc. Am. J.* <https://doi.org/10.2136/sssaj1982.03615995004600050017x>

Heilmann, S.M., Molde, J.S., Timler, J.G., Wood, B.M., Mikula, A.L., Vozhdayev, G. V., Colosky, E.C., Spokas, K.A., Valentas, K.J., 2014. Phosphorus reclamation through hydrothermal carbonization of animal manures. *Environ. Sci. Technol.* <https://doi.org/10.1021/es501872k>

Huang, R., Tang, Y., 2016. Evolution of phosphorus complexation and mineralogy during (hydro)thermal treatments of activated and anaerobically digested sludge:



- Insights from sequential extraction and P K-edge XANES. *Water Res.* 100, 439–447. <https://doi.org/10.1016/j.watres.2016.05.029>
- Huo, S., Liu, J., Addy, M., Chen, P., Necas, D., Cheng, P., Li, K., Chai, H., Liu, Y., Ruan, R., 2020. The influence of microalgae on vegetable production and nutrient removal in greenhouse hydroponics. *J. Clean. Prod.*  
<https://doi.org/10.1016/j.jclepro.2019.118563>
- Idowu, I., Li, L., Flora, J.R.V., Pellechia, P.J., Darko, S.A., Ro, K.S., Berge, N.D., 2017. Hydrothermal carbonization of food waste for nutrient recovery and reuse. *Waste Manag.* 69, 480–491. <https://doi.org/10.1016/j.wasman.2017.08.051>
- Koppelaar, R.H.E.M., Weikard, H.P., 2013. Assessing phosphate rock depletion and phosphorus recycling options. *Glob. Environ. Chang.*  
<https://doi.org/10.1016/j.gloenvcha.2013.09.002>
- Lachos-Perez, D., Brown, A.B., Mudhoo, A., Martinez, J., Timko, M.T., Rostagno, M.A., Forster-Carneiro, T., 2017. Applications of subcritical and supercritical water conditions for extraction, hydrolysis, gasification, and carbonization of biomass: A critical review. *Biofuel Res. J.*  
<https://doi.org/10.18331/BRJ2017.4.2.6>
- Lee, E.K., Zhang, X., Adler, P.R., Kleppel, G.S., Romeiko, X.X., 2020. Spatially and temporally explicit life cycle global warming, eutrophication, and acidification impacts from corn production in the U.S. Midwest. *J. Clean. Prod.*  
<https://doi.org/10.1016/j.jclepro.2019.118465>
- Li, B., Yin, T., Udugama, I.A., Dong, S.L., Yu, W., Huang, Y.F., Young, B., 2020.

- Food waste and the embedded phosphorus footprint in China. *J. Clean. Prod.*  
<https://doi.org/10.1016/j.jclepro.2019.119909>
- Li, H., Li, Y., Xu, Y., Lu, X., 2020. Biochar phosphorus fertilizer effects on soil phosphorus availability. *Chemosphere.*  
<https://doi.org/10.1016/j.chemosphere.2019.125471>
- Li, L., Pan, G., 2013. A universal method for flocculating harmful algal blooms in marine and fresh waters using modified sand. *Environ. Sci. Technol.*  
<https://doi.org/10.1021/es305234d>
- Liu, Xuewei, Yuan, Z., Liu, Xin, Zhang, Y., Hua, H., Jiang, S., 2020. Historic Trends and Future Prospects of Waste Generation and Recycling in China's Phosphorus Cycle. *Environ. Sci. Technol.* <https://doi.org/10.1021/acs.est.9b05120>
- Lu, H., Yan, M., Wong, M.H., Mo, W.Y., Wang, Y., Chen, X.W., Wang, J.J., 2020. Effects of biochar on soil microbial community and functional genes of a landfill cover three years after ecological restoration. *Sci. Total Environ.*  
<https://doi.org/10.1016/j.scitotenv.2020.137133>
- Luo, L. zao, Shao, Y., Luo, S., Zeng, F. jian, Tian, G. ming, 2019. Nutrient removal from piggery wastewater by *Desmodesmus* sp.CHX1 and its cultivation conditions optimization. *Environ. Technol. (United Kingdom).*  
<https://doi.org/10.1080/09593330.2018.1449903>
- Machado, J., Campos, A., Vasconcelos, V., Freitas, M., 2017. Effects of microcystin-LR and cylindrospermopsin on plant-soil systems: A review of their relevance for agricultural plant quality and public health. *Environ. Res.*

<https://doi.org/10.1016/j.envres.2016.09.015>

Mujtaba, G., Rizwan, M., Lee, K., 2017. Removal of nutrients and COD from wastewater using symbiotic co-culture of bacterium *Pseudomonas putida* and immobilized microalga *Chlorella vulgaris*. *J. Ind. Eng. Chem.*

<https://doi.org/10.1016/j.jiec.2017.01.021>

Mukherjee, C., Chowdhury, R., Ray, K., 2015. Phosphorus recycling from an unexplored source by polyphosphate accumulating microalgae and cyanobacteria-a step to phosphorus security in agriculture. *Front. Microbiol.* 6,

1–7. <https://doi.org/10.3389/fmicb.2015.01421>

Oita, A., Wirasenjaya, F., Liu, J., Webeck, E., Matsubae, K., 2020. Trends in the food nitrogen and phosphorus footprints for Asia's giants: China, India, and Japan. *Resour. Conserv. Recycl.* 157, 104752.

<https://doi.org/10.1016/j.resconrec.2020.104752>

Pan, G., Lyu, T., Mortimer, R., 2018. Comment: Closing phosphorus cycle from natural waters: re-capturing phosphorus through an integrated water-energy-food strategy. *J. Environ. Sci. (China)*. <https://doi.org/10.1016/j.jes.2018.02.018>

Powell, N., Shilton, A., Chisti, Y., Pratt, S., 2009. Towards a luxury uptake process via microalgae - Defining the polyphosphate dynamics. *Water Res.*

<https://doi.org/10.1016/j.watres.2009.06.011>

Prasad, P., Pullar, D., Pratt, S., 2014. Facilitating access to the algal economy: Mapping waste resources to identify suitable locations for algal farms in Queensland. *Resour. Conserv. Recycl.*

<https://doi.org/10.1016/j.resconrec.2014.01.008>

Ray, K., Mukherjee, C., Ghosh, A.N., 2013. A way to curb phosphorus toxicity in the environment: Use of polyphosphate reservoir of cyanobacteria and microalga as a safe alternative phosphorus biofertilizer for Indian agriculture. *Environ. Sci. Technol.* 47, 11378–11379. <https://doi.org/10.1021/es403057c>

Santos, F.M., Pires, J.C.M., 2018. Nutrient recovery from wastewaters by microalgae and its potential application as bio-char. *Bioresour. Technol.* 267, 725–731. <https://doi.org/10.1016/j.biortech.2018.07.119>

Schreiber, C., Schiedung, H., Harrison, L., Briese, C., Ackermann, B., Kant, J., Schrey, S.D., Hofmann, D., Singh, D., Ebenhöf, O., Amelung, W., Schurr, U., Mettler-Altmann, T., Huber, G., Jablonowski, N.D., Nedbal, L., 2018. Evaluating potential of green alga *Chlorella vulgaris* to accumulate phosphorus and to fertilize nutrient-poor soil substrates for crop plants. *J. Appl. Phycol.* <https://doi.org/10.1007/s10811-018-1390-9>

Sha, Z., Chen, Z., Feng, Y., Xue, L., Yang, L., Cao, L., Chu, Q., 2020. Minerals loaded with oxygen nanobubbles mitigate arsenic translocation from paddy soils to rice. *J. Hazard. Mater.* <https://doi.org/10.1016/j.jhazmat.2020.122818>

Sha, Z., Watanabe, T., Chu, Q., Oka, N., Osaki, M., Shinano, T., 2018. A Reduced Phosphorus Application Rate Using a Mycorrhizal Plant as the Preceding Crop Maintains Soybean Seeds' Nutritional Quality. *J. Agric. Food Chem.* [acs.jafc.8b05288. https://doi.org/10.1021/acs.jafc.8b05288](https://doi.org/10.1021/acs.jafc.8b05288)

Shen, J., Yuan, L., Zhang, J., Li, H., Bai, Z., Chen, X., Zhang, W., Zhang, F., 2011.

Phosphorus dynamics: From soil to plant. *Plant Physiol.* 156, 997–1005.

<https://doi.org/10.1104/pp.111.175232>

Shen, Q., Wen, Z., Dong, Y., Li, H., Miao, Y., Shen, J., 2018. The responses of root morphology and phosphorus-mobilizing exudations in wheat to increasing shoot phosphorus concentration. *AoB Plants*. <https://doi.org/10.1093/aobpla/ply054>

Shen, Y., Gao, J., Li, L., 2017. Municipal wastewater treatment via co-immobilized microalgal-bacterial symbiosis: Microorganism growth and nutrients removal.

*Bioresour. Technol.* <https://doi.org/10.1016/j.biortech.2017.07.041>

Solovchenko, A., Khozin-Goldberg, I., Selyakh, I., Semenova, L., Ismagulova, T., Lukyanov, A., Mamedov, I., Vinogradova, E., Karpova, O., Konyukhov, I., Vasilieva, S., Mojzes, P., Dijkema, C., Vecherskaya, M., Zvyagin, I., Nedbal, L., Gorelova, O., 2019. Phosphorus starvation and luxury uptake in green microalgae revisited. *Algal Res.* <https://doi.org/10.1016/j.algal.2019.101651>

Solovchenko, A., Verschoor, A.M., Jablonowski, N.D., Nedbal, L., 2016. Phosphorus from wastewater to crops: An alternative path involving microalgae. *Biotechnol. Adv.* 34, 550–564. <https://doi.org/10.1016/j.biotechadv.2016.01.002>

Subramaniam, V., Subashchandrabose, S.R., Ganeshkumar, V., Thavamani, P., Chen, Z., Naidu, R., Megharaj, M., 2016. Cultivation of *Chlorella* on brewery wastewater and nano-particle biosynthesis by its biomass. *Bioresour. Technol.* 211, 698–703. <https://doi.org/10.1016/j.biortech.2016.03.154>

Tao, R., Kinnunen, V., Praveenkumar, R., Lakaniemi, A.M., Rintala, J.A., 2017. Comparison of *Scenedesmus acuminatus* and *Chlorella vulgaris* cultivation in

- liquid digestates from anaerobic digestion of pulp and paper industry and municipal wastewater treatment sludge. *J. Appl. Phycol.*  
<https://doi.org/10.1007/s10811-017-1175-6>
- Václavková, Š., Šyc, M., Moško, J., Pohořelý, M., Svoboda, K., 2018. Fertilizer and Soil Solubility of Secondary P Sources - The Estimation of Their Applicability to Agricultural Soils. *Environ. Sci. Technol.*  
<https://doi.org/10.1021/acs.est.8b02105>
- Wang, T., Camps-Arbestain, M., Hedley, M., 2014. The fate of phosphorus of ash-rich biochars in a soil-plant system. *Plant Soil.*  
<https://doi.org/10.1007/s11104-013-1938-z>
- Wang, Tao, Zhai, Y., Zhu, Y., Peng, C., Wang, Tengfei, Xu, B., Li, C., Zeng, G., 2017. Feedwater pH affects phosphorus transformation during hydrothermal carbonization of sewage sludge. *Bioresour. Technol.* 245, 182–187.  
<https://doi.org/10.1016/j.biortech.2017.08.114>
- Withers, P.J.A., Forber, K.G., Lyon, C., Rothwell, S., Doody, D.G., Jarvie, H.P., Martin-Ortega, J., Jacobs, B., Cordell, D., Patton, M., Camargo-Valero, M.A., Cassidy, R., 2020. Towards resolving the phosphorus chaos created by food systems. *Ambio.* <https://doi.org/10.1007/s13280-019-01255-1>
- Xu, G., Zhang, Y., Shao, H., Sun, J., 2016. Pyrolysis temperature affects phosphorus transformation in biochar: Chemical fractionation and <sup>31</sup>P NMR analysis. *Sci. Total Environ.* <https://doi.org/10.1016/j.scitotenv.2016.06.081>
- Xu, H.J., Wang, X.H., Li, H., Yao, H.Y., Su, J.Q., Zhu, Y.G., 2014. Biochar impacts

- soil microbial community composition and nitrogen cycling in an acidic soil planted with rape. *Environ. Sci. Technol.* <https://doi.org/10.1021/es5021058>
- Xu, M., Gao, P., Yang, Z., Su, L., Wu, J., Yang, G., Zhang, X., Ma, J., Peng, H., Xiao, Y., 2019. Biochar impacts on phosphorus cycling in rice ecosystem. *Chemosphere* 225, 311–319. <https://doi.org/10.1016/j.chemosphere.2019.03.069>
- Yao, Y., Gao, B., Chen, J., Yang, L., 2013. Engineered biochar reclaiming phosphate from aqueous solutions: Mechanisms and potential application as a slow-release fertilizer. *Environ. Sci. Technol.* 47, 8700–8708. <https://doi.org/10.1021/es4012977>
- Ye, S., Zeng, G., Wu, H., Liang, J., Zhang, C., Dai, J., Xiong, W., Song, B., Wu, S., Yu, J., 2019. The effects of activated biochar addition on remediation efficiency of co-composting with contaminated wetland soil. *Resour. Conserv. Recycl.* <https://doi.org/10.1016/j.resconrec.2018.10.004>
- Yu, S., Feng, Y., Xue, L., Sun, H., Han, L., Yang, L., Sun, Q., Chu, Q., 2019. Biowaste to treasure: Application of microbial-aged hydrochar in rice paddy could improve nitrogen use efficiency and rice grain free amino acids. *J. Clean. Prod.* 240, 118180. <https://doi.org/10.1016/j.jclepro.2019.118180>
- Yu, S., Xue, L., Feng, Y., Liu, Y., Song, Z., Mandal, S., Yang, L., Sun, Q., Xing, B., 2020. Hydrochar reduced NH<sub>3</sub> volatilization from rice paddy soil: Microbial-aging rather than water-washing is recommended before application. *J. Clean. Prod.* 122233. <https://doi.org/10.1016/j.jclepro.2020.122233>
- Yuan, T., Cheng, Y., Huang, W., Zhang, Z., Lei, Z., Shimizu, K., Utsumi, M., 2018.

Fertilizer potential of liquid product from hydrothermal treatment of swine manure. *Waste Manag.* 77, 166–171.

<https://doi.org/10.1016/j.wasman.2018.05.018>

Zhang, H., Chen, C., Gray, E.M., Boyd, S.E., Yang, H., Zhang, D., 2016. Roles of biochar in improving phosphorus availability in soils: A phosphate adsorbent and a source of available phosphorus. *Geoderma*.

<https://doi.org/10.1016/j.geoderma.2016.04.020>

Journal Pre-proof



## Captions to illustrations

**Table 1.** Basic physiochemical characteristics of raw microalgae and microalgae-derived hydrochars.

**Table 2.** Hydrochar yield, total P content and P recovery of the microalgae-derived hydrochars (n=3).

**Figure 1.** Growth curves of *Chlorella vulgaris* and *Microcystis sp.* and dynamic variation of P concentration in poultry farm wastewater.

**Figure 2.** Fractionation of P in sequential extracts of raw microalgae and microalgae-derived hydrochars.

**Figure 3.** The dynamic variation of soil available P with the application of chemical fertilizer, raw microalgae and microalgae-derived hydrochars during 120 days incubation.

**Figure 4.** P fractionation in the rhizosphere soil grown with wheat, including (A) soluble P fraction, (B) exchangeable P fraction, (C) Fe/Al-bound P fraction, (D) Ca-bound P fraction, and (E) residual P fraction.

**Figure 5.** Wheat PUE (A) and grain yield (B) in a pot experiment. Each value was the average of results from four replicates.

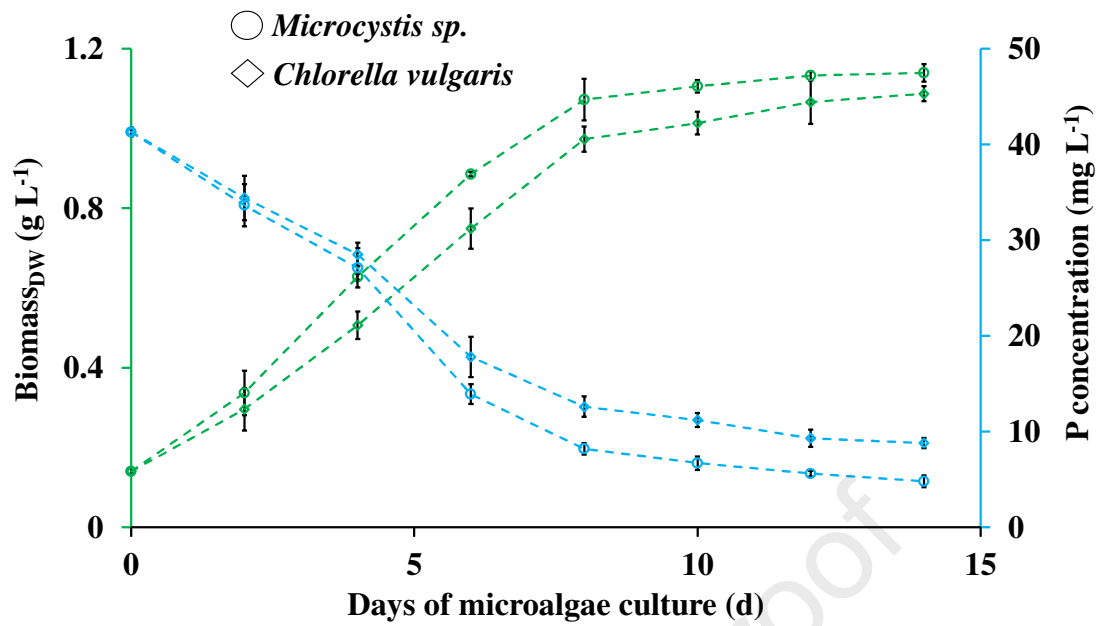
**Table 1.** Basic physiochemical characteristics of raw microalgae and microalgae-derived hydrochars. Values are means  $\pm$  SE of three independent measurements.

|                                                    | CV             | CVHW200        | CVHW260        | CVHCA200       | CVHCA260       | MS              | MSHW200         | MSHW260        | MSHCA200       | MSHCA260        |
|----------------------------------------------------|----------------|----------------|----------------|----------------|----------------|-----------------|-----------------|----------------|----------------|-----------------|
| pH <sup>a</sup>                                    | 8.2 $\pm$ 0.3  | 7.4 $\pm$ 0.2  | 7.6 $\pm$ 0.4  | 6.1 $\pm$ 0.1  | 6.5 $\pm$ 0.1  | 8.0 $\pm$ 0.5   | 7.9 $\pm$ 0.3   | 8.3 $\pm$ 0.2  | 5.9 $\pm$ 0.2  | 6.4 $\pm$ 0.1   |
| C (%) <sup>b</sup>                                 | 63.8 $\pm$ 2.9 | 55.6 $\pm$ 3.5 | 56.4 $\pm$ 1.8 | 60.5 $\pm$ 5.7 | 59.3 $\pm$ 2.4 | 65.6 $\pm$ 1.8  | 58.7 $\pm$ 3.6  | 57.2 $\pm$ 3.2 | 60.3 $\pm$ 6.4 | 61.0 $\pm$ 3.7  |
| H (%)                                              | 4.1 $\pm$ 0.2  | 4.1 $\pm$ 0.4  | 4.4 $\pm$ 0.2  | 3.3 $\pm$ 0.1  | 3.8 $\pm$ 0.3  | 4.0 $\pm$ 0.1   | 3.8 $\pm$ 0.1   | 3.4 $\pm$ 0.1  | 3.0 $\pm$ 0.1  | 3.2 $\pm$ 0.2   |
| N (%)                                              | 10.8 $\pm$ 0.4 | 8.7 $\pm$ 0.7  | 7.3 $\pm$ 0.6  | 8.1 $\pm$ 0.4  | 6.2 $\pm$ 0.5  | 12.3 $\pm$ 0.7  | 10.2 $\pm$ 0.4  | 9.2 $\pm$ 0.6  | 9.5 $\pm$ 1.1  | 8.8 $\pm$ 0.7   |
| S (%)                                              | 2.7 $\pm$ 0.2  | 1.5 $\pm$ 0.1  | 0.4 $\pm$ 0.03 | 1.4 $\pm$ 0.1  | 0.8 $\pm$ 0.09 | 2.2 $\pm$ 0.2   | 1.3 $\pm$ 0.03  | 0.6 $\pm$ 0.04 | 1.5 $\pm$ 0.1  | 0.6 $\pm$ 0.03  |
| K (%)                                              | 1.8 $\pm$ 0.1  | 1.5 $\pm$ 0.2  | 1.1 $\pm$ 0.1  | 1.3 $\pm$ 0.07 | 0.9 $\pm$ 0.05 | 1.6 $\pm$ 0.2   | 1.2 $\pm$ 0.1   | 1.3 $\pm$ 0.06 | 1.1 $\pm$ 0.2  | 0.8 $\pm$ 0.04  |
| Al (%)                                             | 0.8 $\pm$ 0.05 | 1.1 $\pm$ 0.2  | 1.2 $\pm$ 0.2  | 1.8 $\pm$ 0.3  | 1.9 $\pm$ 0.3  | 1.0 $\pm$ 0.1   | 1.7 $\pm$ 0.2   | 1.7 $\pm$ 0.1  | 2.2 $\pm$ 0.3  | 2.4 $\pm$ 0.4   |
| Ca (%)                                             | 1.1 $\pm$ 0.07 | 1.3 $\pm$ 0.2  | 1.5 $\pm$ 0.1  | 2.2 $\pm$ 0.3  | 2.4 $\pm$ 0.2  | 0.9 $\pm$ 0.08  | 1.2 $\pm$ 0.1   | 1.3 $\pm$ 0.2  | 1.8 $\pm$ 0.08 | 2.1 $\pm$ 0.3   |
| Fe (%)                                             | 0.7 $\pm$ 0.04 | 0.9 $\pm$ 0.1  | 1.1 $\pm$ 0.06 | 1.5 $\pm$ 0.1  | 1.6 $\pm$ 0.2  | 0.4 $\pm$ 0.03  | 0.8 $\pm$ 0.05  | 0.8 $\pm$ 0.08 | 1.3 $\pm$ 0.1  | 1.5 $\pm$ 0.06  |
| Mg (%)                                             | 0.1 $\pm$ 0.02 | 0.3 $\pm$ 0.04 | 0.4 $\pm$ 0.02 | 0.6 $\pm$ 0.05 | 0.6 $\pm$ 0.04 | 0.08 $\pm$ 0.01 | 0.1 $\pm$ 0.007 | 0.2 $\pm$ 0.04 | 0.4 $\pm$ 0.03 | 0.05 $\pm$ 0.06 |
| SSA (m <sup>2</sup> g <sup>-1</sup> ) <sup>c</sup> | 0.6 $\pm$ 0.02 | 5.4 $\pm$ 0.05 | 5.7 $\pm$ 0.02 | 6.6 $\pm$ 0.07 | 6.4 $\pm$ 0.06 | 0.4 $\pm$ 0.04  | 5.2 $\pm$ 0.04  | 5.0 $\pm$ 0.06 | 5.9 $\pm$ 0.06 | 6.1 $\pm$ 0.05  |
| Porosity<br>(cm <sup>3</sup> g <sup>-1</sup> )     | 0.004 $\pm$    | 0.05 $\pm$     | 0.03 $\pm$     | 0.06 $\pm$     | 0.04 $\pm$     | 0.002 $\pm$     | 0.03 $\pm$      | 0.02 $\pm$     | 0.04 $\pm$     | 0.03 $\pm$      |

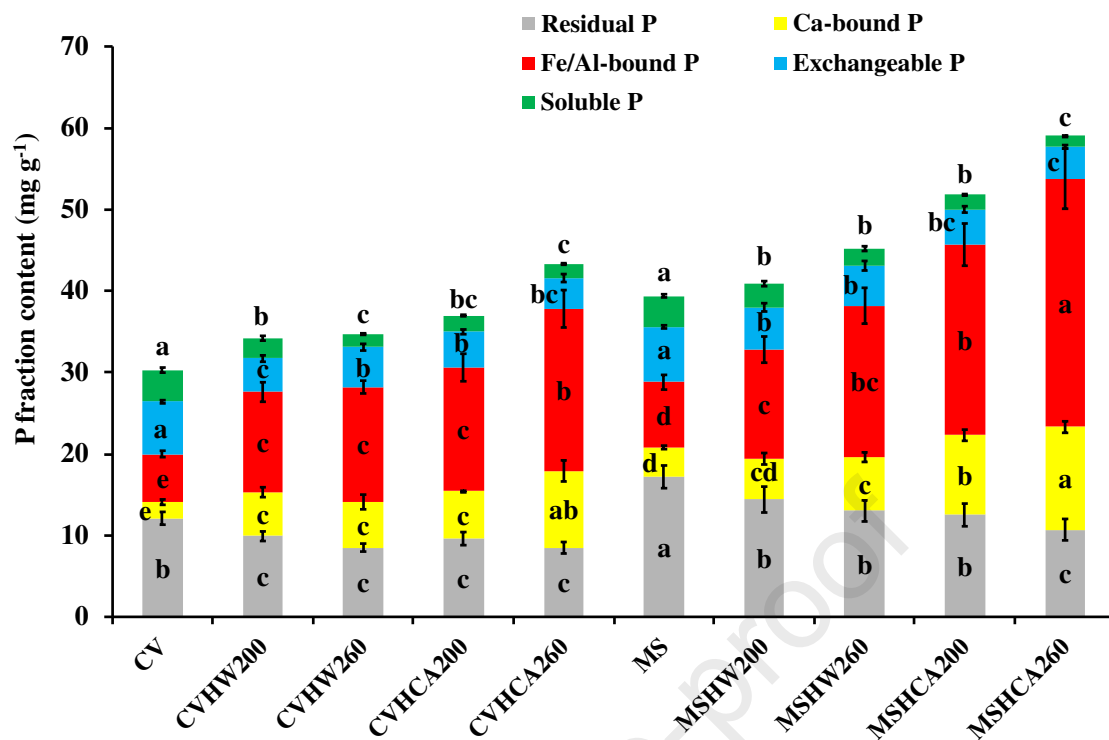
- The pH was determined by a pH meter using a solid/Milli-Q water ratio of 1:2.5 (w/v).
- The total elemental concentrations of C, H, N, and S were determined by an Elemental Analyzer (EL III; Elementar Analysensysteme GmbH, Germany). The total concentrations of elemental Al, Ca, Fe, and Mg were measured using ICP-OES.
- SSA and porosity were measured were measured using a NOVA 1200 analyzer (Anton Paar QuantaTec Inc., Graz, Austria), and the parameters were calculated using the Brunauer–Emmett–Teller method.

**Table 2.** Hydrochar yield, total P content and P recovery of the microalgae-derived hydrochars (n=3). (N/A: not applicable)

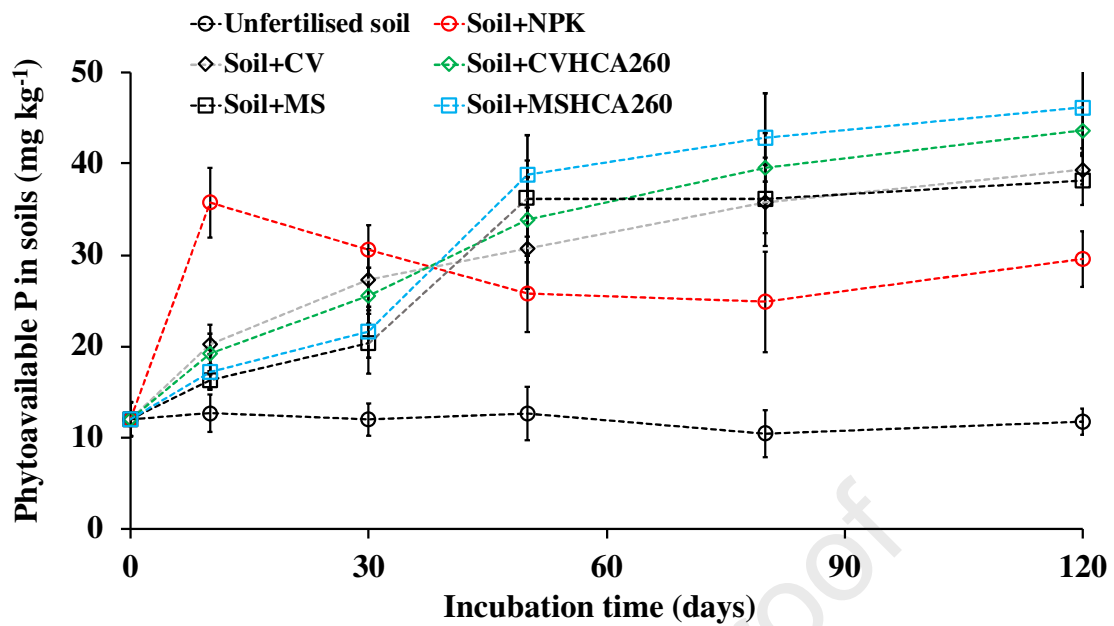
| Feedstock                 | HTC reaction medium        | Sample label | Solid recovery rate (%) | Total P concentration (wt%) | P recovery (%) |
|---------------------------|----------------------------|--------------|-------------------------|-----------------------------|----------------|
| <i>Chlorella vulgaris</i> | Raw                        | CV           | N/A                     | 2.7 ± 0.1                   | N/A            |
|                           | Deionized water, 200 °C    | CVHW200      | 40.7 ± 3.9              | 3.4 ± 0.2                   | 51.3           |
|                           | Deionized water, 260 °C    | CVHW260      | 37.3 ± 5.0              | 3.6 ± 0.1                   | 49.7           |
|                           | 1 wt.% citric acid, 200 °C | CVHCA200     | 49.8 ± 3.7              | 3.8 ± 0.3                   | 70.1           |
|                           | 1 wt.% citric acid, 260 °C | CVHCA260     | 45.4 ± 4.3              | 4.3 ± 0.4                   | 72.3           |
| <i>Microcystis sp.</i>    | Raw                        | MS           | N/A                     | 3.5 ± 0.1                   | N/A            |
|                           | Deionized water, 200 °C    | MSHW200      | 44.6 ± 1.7              | 4.2 ± 0.3                   | 53.5           |
|                           | Deionized water, 260 °C    | MSHW260      | 42.1 ± 5.4              | 4.8 ± 0.3                   | 57.4           |
|                           | 1 wt.% citric acid, 200 °C | MSHCA200     | 58.8 ± 3.2              | 5.2 ± 0.2                   | 87.4           |
|                           | 1 wt.% citric acid, 260 °C | MSHCA260     | 55.2 ± 2.8              | 5.8 ± 0.4                   | 91.5           |



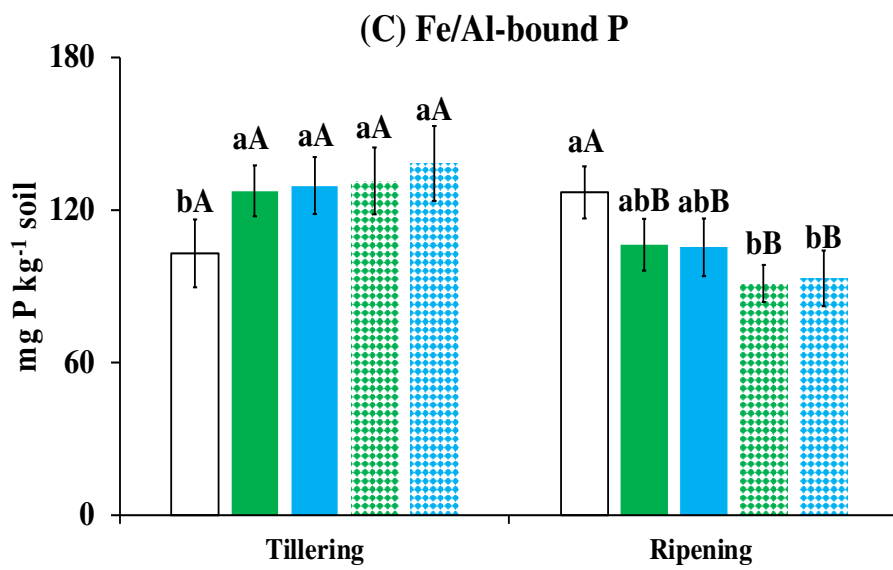
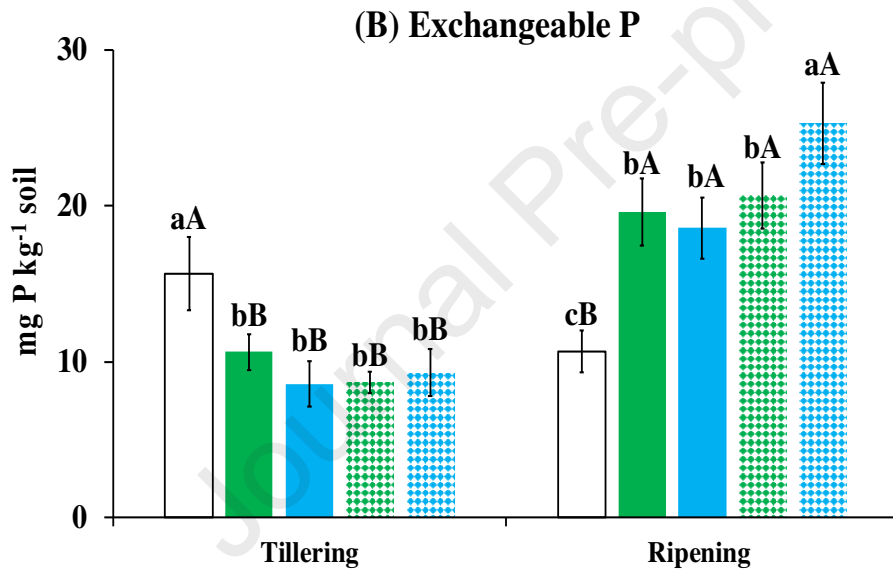
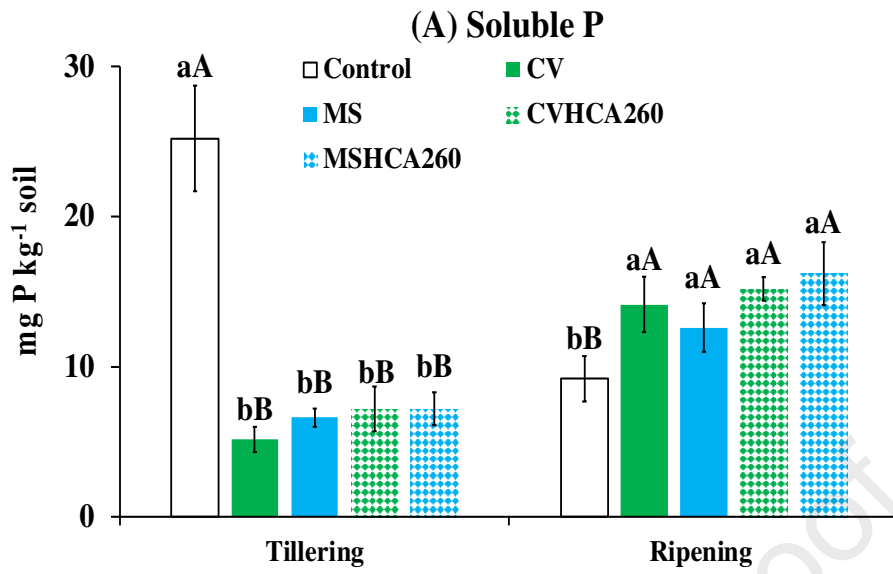
**Figure 1.** Growth curves of *Chlorella vulgaris* and *Microcystis sp.* and dynamic variation of P concentration in poultry farm wastewater. Green circles and diamonds represent the biomass and blue markers represent the P concentration in the wastewater. Values are means  $\pm$  SE of three independent measurements. The biomass was based on the dry weight (DW) of microalgae.



**Figure 2.** Fractionation of P in sequential extracts of raw microalgae and microalgae-derived hydrochars. Each data was the average of results from three independent extraction experiments. Error bars indicate SE. Means not sharing the same letter (a-e) are significantly different at the  $p = 0.05$  level by one-way ANOVA. The abbreviations of materials are the same as those in Table 2. The relative abundance (percentage) of each P fractionation is shown in Table S2.



**Figure 3.** The dynamic variation of soil available P with the application of chemical fertilizer, raw microalgae and microalgae-derived hydrochars during 120 days incubation. Each data was the average of results from four replicates. Error bars indicate SE (n = 4). Significant differences between treatments are indicated with different letters. The abbreviations of materials are the same as those in Table 2. Soil+NPK means the soil applied with chemical N, P, and K fertilizers.



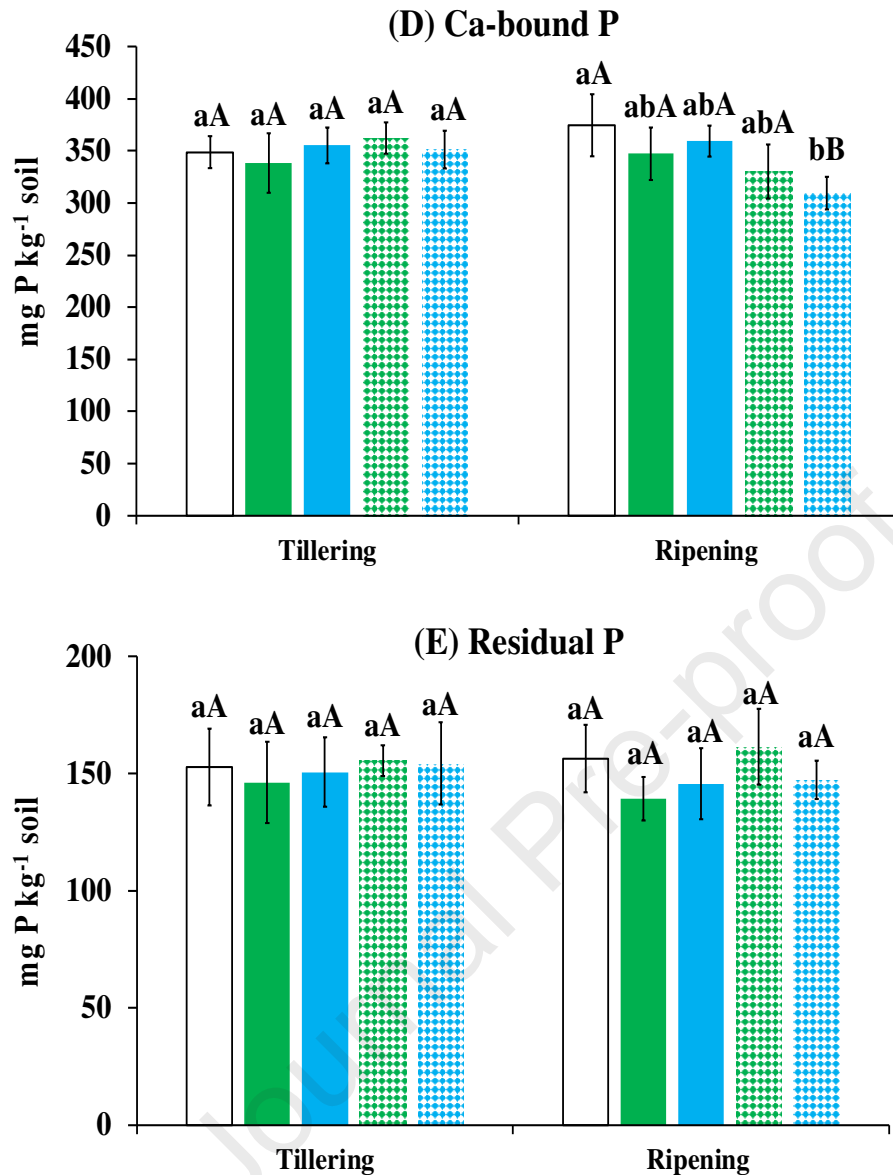


**Figure 4.** P fractionation in the rhizosphere soil grown with wheat, including (A) soluble P fraction, (B) exchangeable P fraction, (C) Fe/Al-bound P fraction, (D) Ca-bound P fraction, and (E) residual P fraction. Each data was the average of results from four replicates. Error bars indicate SE (n = 4). Columns denoted by different lowercase letters indicate statistically significant differences affected by different microalgae and microalgae-derived hydrochar treatments, and those labelled with different uppercase letters indicate significant differences for the same treatment between tillering and ripening stages. The abbreviations of materials are the same as those in **Table 2**. The sequential extraction method and explanation of different P fractions are detailed in **Fig S2**. The results of labile P pool and stable P pool are shown in **Fig S5**.



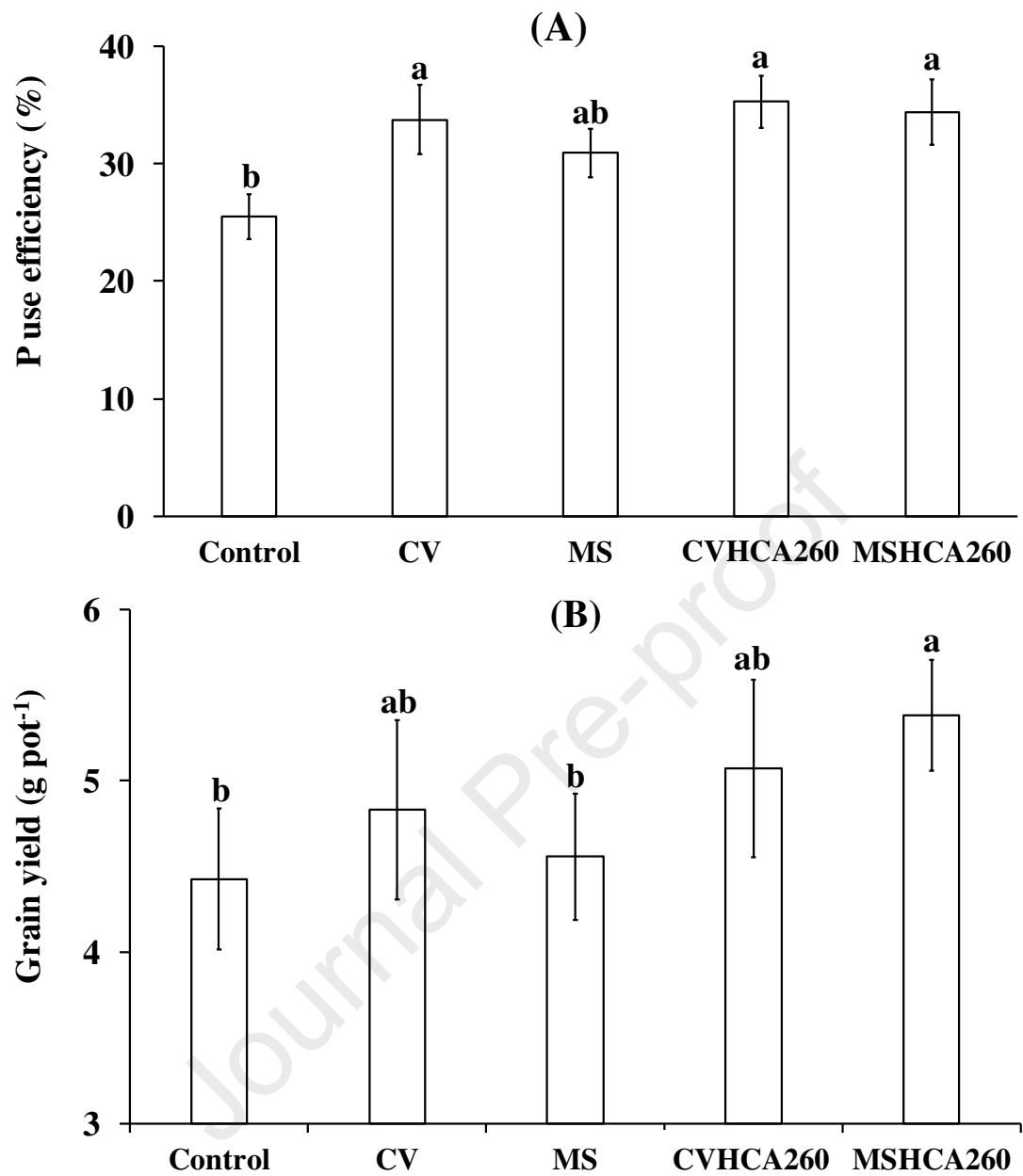


**Figure 5.** Wheat PUE (A) and grain yield (B) in a pot experiment. Each value was the average of results from four replicates. Error bars indicate SE (n = 4). Statistically significant differences between treatments are indicated with different letters. The abbreviations of materials are those detailed in **Table 2**.

## Highlights

- *Chlorella vulgaris* and *Microcystis sp.* (MS) removed 78.7% and 88.4% phosphorous (P)
- 91.5% P was recovered from MS to MS-derived hydrochar produced at 260 °C (MSHCA260)
- Microalgal hydrochars slowly released P and improved soil P availability
- MSHCA260 increased P use efficiency and wheat yield compared to chemical fertilizer
- Microalgae and hydrochar technology recycled P from wastewater to crop food

## **Credit author statement**

QC designed the experiments; GP and LX acquired the funding and supervised the research; QC, TL, BY, and MC performed the experiments; QC analyzed the data; YF and LY visualized the work; QC wrote the manuscript; TL, RM, LY, and MC reviewed and edited the manuscript; QC, GP, and LX finalized the manuscript.

Journal Pre-proof

**Declaration of interests**

The authors declare that they have no known competing financial interests or personal relationships that could have appeared to influence the work reported in this paper.

The authors declare the following financial interests/personal relationships which may be considered as potential competing interests:

Journal Pre-proof

# Hydrothermal carbonization of microalgae for phosphorus recycling from wastewater to crop-soil systems as slow-release fertilizers

Chu, Qingnan

2020-10-12

Attribution-NonCommercial-NoDerivatives 4.0 International

---

Chu Q, Lyu T, Xue L, et al., (2021) Hydrothermal carbonization of microalgae for phosphorus recycling from wastewater to crop-soil systems as slow-release fertilizers. *Journal of Cleaner Production*, Volume 283, February 2021, Article number 124627

<https://doi.org/10.1016/j.jclepro.2020.124627>

*Downloaded from CERES Research Repository, Cranfield University*